An edited version of this paper was published by AGU
**JOURNAL OF GEOPHYSICAL RESEARCH**
DEC 2004; VOL 109; PART 12; SECT 3; pp. C12037
http://dx.doi.org/10.1029/2003JC002145




# Hydrology and circulation in the Strait of Hormuz and the Gulf of Oman—Results from the GOGP99 Experiment: 1. Strait of Hormuz

S. P. Pous[1,*], X. Carton[1], P. Lazure[2]

1 : Laboratoire de Physique des Océans, IFREMER/CNRS/UBO, Brest, France
2 : Direction de l'Environnement et de l'aménagement Littoral, Applications Opérationnelles, IFREMER, Plouzané, France

*: Corresponding author : Stephane.Pous@ifremer.fr

**Abstract:**

In October and early November 1999, the GOGP99 experiment collected hydrological, currentmeter, tide recorder, thermistor and drifting buoy data near the Strait of Hormuz. Data analysis provides the water mass structure in the Strait: Persian Gulf Water (PGW) core is banked against the Omani coast, while Indian Ocean Surface Water (IOSW) lies near the Iranian coast. These water masses are most often covered by a homogeneous surface layer. Thermohaline characteristics of the PGW core decrease substantially downstream, from the Persian/Arabian Gulf to the Gulf of Oman. PGW and IOSW thermohaline characteristics and distribution also exhibit notable changes at periods shorter than a month as shown by repeated hydrological sections. The tidal signal measured south of the Strait by moored ADCP and thermistor chains has predominant semi-diurnal M2 and S2 and diurnal K1 components and possesses a complex vertical structure. Tidal intensification near the surface pycnocline is associated with noticeable internal waves. At subtidal timescale, mooring recordings confirm the water mass variability observed in the repeated hydrological sections. The mixed layer also deepens substantially during the 1-month period. Finally, trajectories of surface buoys drogued at 15 m exhibit reversals over periods characteristic of changes in wind direction.

# Hydrology and circulation in the Strait of Hormuz and the Gulf of Oman; results from the GOGP99 Experiment. Part I. Strait of Hormuz

S. P. Pous, X. Carton, P. Lazure

## abstract

In October and early November 1999, the GOGP99 experiment collected hydrological, currentmeter, tide recorder, thermistor and drifting buoy data near the Strait of Hormuz. Data analysis provides the water mass structure in the Strait : Persian Gulf Water (PGW) core is banked against the Omani coast, while Indian Ocean Surface Water (IOSW) lies near the Iranian coast. These water masses are most often covered by a homogeneous surface layer. Thermohaline characteristics of the PGW core decrease substantially downstream, from the Persian/Arabian Gulf to the Gulf of Oman. PGW and IOSW thermohaline characteristics and distribution also exhibit notable changes at periods shorter than a month as shown by repeated hydrological sections. The tidal signal measured south of the Strait by moored ADCP and thermistor chains has predominant semi-diurnal M2 and S2 and diurnal K1 components and possesses a complex vertical structure. Tidal intensification near the surface pycnocline is associated with noticeable internal waves. At subtidal time scale, mooring recordings confirm the water mass variability observed in the repeated hydrological sections. The mixed layer also deepens substantially during the one-month period. Finally, trajectories of surface buoys drogued at 15m exhibit reversals over periods characteristic of changes in wind direction.

## 1 Introduction

The Arabian/Persian Gulf (hereafter the Gulf) is a shallow semi-enclosed basin (of average depth 35m) connected to the Gulf of Oman through the Strait of Hormuz. The Gulf of Oman opens on the Northwestern Indian Ocean and on the Arabian Sea. The general orientation of the two gulfs is northwest-southeast; the Gulf extends between 24 and $30^oN$ and 48 and $56^oE$ and is $L$-shaped, the Gulf of Oman is located between 22 and $26^oN$ and 56 and $62^oE$ (see Figure 1). Maximum depth in the Gulf is 90m (see also Johns, 2003), except in the Straits of Hormuz where depths in excess of 100m are found. On the contrary, the 200m isobath remains close to the coasts in the Gulf of Oman where depths larger than 3000m are found (see Figure 2). The Strait of Hormuz is 56km wide and roughly 90m deep but for a trough near and around the Musandam Peninsula. Atmospheric conditions over these two gulfs are northwesterly winds, with seasonal variations over the Gulf of Oman, high pressures in winter (1015 hPa) with relative low in summer (995 hPa) and air temperatures varying between $32 - 34^oC$ in summer and $18 - 20^oC$ in winter. The region is arid leading to substantial evaporation, greatly exceeding precipitation and river discharge. The evaporation rate was estimated by various authors within [1.44, 2.0] m $yr^{-1}$ (Privett, 1959; Meshal et al, 1986; Chao et al., 1992) whereas river run-off was estimated at [0.15, 0.46] m $yr^{-1}$ (Hartmann et al., 1971; Reynolds, 1993) and precipitation rate at [0.07, 0.1] m $yr^{-1}$ (Hartmann et al., 1971; Reynolds, 1993).

The shallowness of the Gulf, the high evaporation rate, combined with a limited exchange through the Strait of Hormuz cause the formation of a salty and dense water mass called Persian Gulf Water (PGW) and the Gulf to act as an inverse estuary with a relatively fresher surface water inflow from Indian Ocean (IOSW). The limited available data show that the PGW outflow is confined to the western part of the Strait and that the IOSW flows into the Gulf along the eastern part of the Strait and follows the Iranian coast northwards. Values of transport of PGW and IOSW through the Strait are in the range $[0.1, 0.25]Sv$ (Ahmad and Sultan, 1990; Bower et al., 2000; Johns et al., 2003). However, data show high variability regarding these features (Sultan and Elghribi, 1996; Bower et al., 2000; Swift and Bower, 2003) and suggest that complex processes govern the water exchange through the Strait. In particular, Bower et al. (2000) and Swift and Bower (2003) studied the seasonal variability of the formation of dense PGW outflow and the surrounding oceanic environment with temperature and salinity profiles from MOODS[1] at NAVOCEANO[2]. This study found an outflow salinity slightly lower in winter ($\sim$0.5 psu) than in summer and a temperature cooler by about $3^oC$ in winter. Johns et al. (2003) observed a winter-summer difference in PGW outflow temperature and salinity of $-4^oC$ and 1.5 psu ($21^oC$ and 40.8 psu in winter, $25^oC$ and 39.3 psu in summer). Time series of data collected in the Strait of Hormuz in 1996-1997 (Johns et al., ibid) also showed short-term variations of the PGW salinity (up to 1 psu variations over a month), while currents measured in the deeper part of the Strait were found relatively steady (roughly in the [0.2 ; 0.3] m/s range).

Since few data were available on the short term variability of this outflow, and considering that recent studies emphasized the complex dynamics in the Strait of Hormuz area, the French Navy Hydrographic and Oceanographic Service (SHOM) conducted a one month long oceanographic experiment in the Strait of Hormuz and in the Gulf of Oman in October (and early November) 1999; this experiment was called GOGP99. Its aims were to characterize the local hydrological structure and currents and their short-term variability. Hydrological sections in the Strait and the Gulf of Oman were repeated up to three times within that period; unfortunately, due to lack of security clearance, these sections could not be extended into Iranian waters. ADCP, tide recorders and thermistor chains were moored near the Strait and shallow-drogued surface drifters (Surdrift buoys) were released in its vicinity. Other measurements, such as Seasoar or Shipborne ADCP sections, will be presented in Part 2 of this paper. The data are analyzed here to present the hydrology and currents near the Strait, their variability over a few day to two week period and to relate this variability with tidal and atmospheric forcing (inasmuch as possible).

The outline of this paper is as follows: after presenting the data collection and processing, results on the hydrology and currents, and their short-term variability are detailed on five sections in and near the Strait of Hormuz. Then, the time variations of velocity and temperature obtained with moorings and floats south of the Strait of Hormuz are described. Finally the main results are summarized and conclusions are drawn on essential features which should be measured during future experiments.

# 2 Data collection and processing

The GOGP experiment was conducted by SHOM in the Strait of Hormuz and in the Gulf of Oman from October 8 till November 10, 1999. This experiment performed 99 CTD stations or XBT, XCTD casts[3] in and near the Strait of Hormuz, under the form of 5 sections repeated twice or thrice at roughly 10 day interval (see Figure 3 for their location). The

[1] Master Oceanographic Observations Data Set; note that MOODS dataset contains few observations in that region between July and December

[2] US Naval oceanographic Office

[3] Conductivity Temperature Depth or eXpendable BathyThermographs, eXpendable Conductivity Temperature Depth probes

individual contents of each section varied between 4 and 14 soundings (see Table 1). These sections could not be extended into Iranian waters by lack of authorization.

One ADCP mooring and two thermistor chain moorings were set up for one month near the Strait of Hormuz and in the northern part of the Gulf of Oman (see again Figure 2 and see information in Table 2). On mooring D1, the 500 kHz ADCP was fixed near the bottom and data were collected in 4m vertical bins, from the surface down to 115m depth, at 2 minute intervals between October 8 and November 9, 1999. Data analysis showed that current measurements in the upper 20m were not reliable due to too intense an ambient noise; this noise is created by ship propellers in a region with heavy maritime traffic. The thermistor chains (T2 and T3) were moored near the bottom (at 120 and 96m) and data were collected (every 2.5m vertically above 30m depth, and every 5m below), from 3m down to 83m depths, at 5 minute intervals, from October 8 to November 9, 1999.

Two tide recorders were moored near the Strait of Hormuz (M1 in the Gulf, M2 near the ADCP mooring, see position on Figure 2). Tide recorders integrate data over 4 mn intervals and sample data for output every 5 mn.

Finally five surface drifting buoys (Surdrifts) were deployed in and near the Strait, at locations and dates given in Figure 2 and Table 3. The Surdrift buoys were drogued at depths expected to be characteristic of the PGW outflow and of the IOSW inflow, i.e at 85 and at 15m. It appeared that the latter buoys followed motions in the mixed layer (the IOSW lying near 40m depth at the locations where the Surdrifts were released).

Other hydrological measurements, surdrift trajectories, Seasoar and Shipborne ADCP measurements will be described in Part 2 of this paper, since they concern only the Gulf of Oman.

Quality checks, calibration and filtering were applied to the data[4].

Hydrological profiles were first calibrated on in-situ measurements (surface temperature and chemical analysis of salinity from water samples). Then, a median filter was applied and spurious points were eliminated by visual inspection of each profile. A Newtonian binomial smoothing was then applied to reduce the number of points to 10 to 20% of initial number, under the condition that the initial (filtered) profile could be reconstructed via linear interpolation with a minimal error. CTD accuracy is $\pm 0.003^oC$, $\pm 0.005$ in salinity, $\pm 1$ dbar. Hydrological sections were visualized within Ocean Data View software (Schlitzer, 2003).

Moored ADCP measurements were first checked after recovery of the instrument. Both mooring depth and compass cape were found stable. Spurious noise was filtered : only data with a signal to noise ratio above $1dB$ were retained, and a one-hour time step was used over a 5-day window for high frequency (tidal) signal. Low frequency variability was obtained by applying a Lanczos filter of rank 288 with a cut-off frequency of 40h. Accuracy on ADCP horizontal velocity data at mooring D1 (at 4m vertical resolution) is $\pm 0.04m/s$. Moored thermistor chain recordings were resampled every 100 minutes. Accuracy on temperatures given by the thermistors is $0.1^oC$.

Moored tide recorders data were first checked visually for spurious values, then filtered and smoothed; harmonic analyses provide results with 1cm precision on amplitudes and $5^o$ accuracy on phases.

Finally, surface drifting (Surdrift) buoys were positioned by GPS with a 100m horizontal accuracy. Trajectories were re-sampled every hour with a three-day window filtering. Tests were performed on acceleration to detect possible loss of drogues or trawling. In such cases, trajectories were ended.

[4]details are given in Vrignaud, Du Reau et al. and Michaux technical reports (2000) which can be obtained from

EPSHOM/CMO, 13 rue du chatellier, 29200 Brest, France

# 3 Hydrology and currents in the vicinity of the Strait of Hormuz

## 3.1 Hydrological features

We describe the hydrological sections from the Gulf outwards to assess the evolution of the Persian Gulf Water outflow. All sections described here are realizations labeled "c" in Table 1, performed on the 1st and 2nd of November 1999.

Figure 4 shows the temperature, salinity and density distributions along section R13 in the Gulf (see Figure 3 for location). Deepest probes reach 80m depth. On most of the section (except perhaps at its northwesternmost point) the hydrological structure consists in a homogeneous mixed layer in the upper 30 meters overlying a stratified water column with the warm and salty PGW core lying in the deepest part of the Strait. The surface homogeneity originates in strong wind and tidal mixing (see Swift and Bower, 2003). The deep PGW core was formed by evaporation and sinking in the Gulf. In the northwestern part of section R13, the weaker vertical temperature and salinity gradients may be associated with a trace of IOSW. Since this section could not extend into Iranian waters, most of the IOSW core was not sampled.
Comparison of temperature and salinity of this section with those of section F of Swift and Bower indicates higher temperatures in November 1999 than in June 1992 (close to $31^oC$ near the surface and $26.5^oC$ near the bottom instead of $29^oC$ and $19^oC$ respectively) but similar salinities (ranging between 37 and 40 psu). This section is closer to that shown in Johns et al. (2003) for July 1997 : this section had surface and bottom temperatures of $31^o$C and $24^o$C and salinities of 37.5 and 39.5 psu.

Section R12 was performed nearly along $56^o30'E$ in the Strait (see Figure 5). Bottom depths range between 50 and 100m with a 260m trough near the northern coast of Musandam Peninsula. The vertical temperature gradient is more marked than that of salinity. The mixed layer is very shallow and lies mostly in the northern part of the section. In the southern part, the salty PGW core was measured between 50m and 220m depths (the station did not probe the water column exactly down to the bottom at 260m); this lower core is associated with strong salinity (maximum 39.5 psu) and nearly homogeneous temperature (close to $27^oC$). This deep core is bounded by a $\sigma_0 = 26kg/m^3$ isopycnal slightly rising towards the coast of Oman.
This thermohaline and density structure is comparable with section C described by Reynolds (1993), though warmer temperatures are observed in November 1999. Hence weaker stratification is found in our dataset (densest waters reached $\sigma_0 = 28kg/m^3$ in June 1992). In the northernmost part of section R12, fresher water seems to indicate the boundary of IOSW inflow near the surface, only marginally sampled by measurements (see also Reynolds, 1993).

Going southward, sections R11, R19 and R18 were performed at the head of the Gulf of Oman, where bottom depths are in the 80-120m range (Figures 6-7-8). These three sections are fairly comparable in structure and show a notable relation between temperature and salinity characteristics, contrary to the previous sections. The western part of each section (R11, R19 and R18) clearly exhibits a three-layer fluid while their eastern part shows only two water masses. In the upper 25m, the well-mixed surface layer has temperature $30^oC$ and salinities between 37 and 37.5 psu. The vertical density gradient separating this mixed layer and the underlying fresher and colder IOSW is strong. IOSW has minimum temperature of $22^oC$ and salinity below 36.5 psu. In the central and western part of the sections, the deepest core is PGW with maximum salinity above 38 psu and temperature above $24^oC$. This important decrease of PGW characteristics from the Gulf (where its salinity was 40psu and it temperature was around $27^o$C) can most likely be attributed to mixing with the IOSW core which lies in its vicinity (in the southern part of the strait). Note that the sharpest decrease in salinity occurs between R19 and R18, as found by Bower et al. (2000).

In straits where currents are subject to high frequency variability, and where barotropic flow may be present, the relevance of geostrophic currents may be weak and their calculation hampered by the choice of a level of reference. Since no ADCP data was available near sections R13 and R12 (indeed moored ADCP D2 did not return data), we use velocity measurements by Johns et al. (2003) on a section close to R13. They provide the vertical profiles of horizontally and annually averaged currents and the horizontally averaged currents for various seasons. Using figure 10a of Johns et al. (ibid) for March 1997, we can see a marked decrease in velocity near 30m depth. This level also lies below the mixed layer. Therefore we choose it as a level of reference. The horizontally and annually averaged velocity at this depth is 0.09 m/s in Johns et al. Thus geostrophic velocities are computed with this level of reference and a 0.09 m/s mean flow is added to the result. The calculated currents perpendicular to section R13b are presented on Figure 9. The outflow velocities are slightly smaller than $0.4m/s$; they are located farther from the Omani coast and deeper than the velocity maxima measured by Johns et al. Surface inflow velocity were smaller than $0.2m/s$, but unfortunately located on the Omani side of the section. In reality maximum inflow of IOSW is expected to lie closer to the Iranian coast and thus has not been sampled.
Though this geostrophic flow is not very accurate, we can nevertheless compute transports for comparison with those calculated by Johns et al. (ibid). Transport T1 is the surface inflow (computed from southwestward flow above 45m depth), T2 is the surface outflow (northeastward upper flow) and T3 the deep outflow (northeastward flow below 45m depth). For R13b, we have T1=0.21 Sv, T2=0.01 Sv and T3=0.16 Sv (compared with 0.23 +/- 0.04 Sv, 0.06 +/- 0.02 Sv, and 0.15 +/- 0.03 Sv for Johns et al.). Changing the level of reference to 10m depth with 0.05 m/s mean flow for the calculation of geostrophic velocity on R13b changed these values to T1=0.18 Sv, T2=0.01 Sv and T3=0.16 Sv. Transports computed on realization (c) of R13 (again with reference level at 30m depth and mean flow of 0.09 m/s) are T1=0.24 Sv, T2=0, T3=0.12 Sv. In summary, transports obtained with our geostrophic velocities (added to a mean flow) are in the range obtained by Johns et al. with an ADCP mooring and the "equivalent width" methodology, except for the surface inflow which is much smaller in our results. Again we believe that most of the surface inflow is concentrated closer to the Iranian coast.

A composite T-S diagram was achieved with sections R11, R19 and R18, showing the three characteristic water masses (mixed layer, IOSW and PGW) and their mixing diagram (Figure 10). Mixing occurs between IOSW and the two adjacent layers (see also the upper part of the T-S diagram in Banse, 1997, for January 1961). Again we note that bottom waters are warmer and lighter in November 1999 than in June 1992 (cf Reynolds, ibid). The $(T, S)$ values of the IOSW show that this core is not sampled on sections R13 and R12, which do not extend to the Iranian coast.

A composite section is made following the most undiluted PGW downstream, along the Strait of Hormuz axis, through sections R13, 12, 11, 19, 18 (see Figure 11). Strong thermal and haline gradients are found between sections R12 and R11s especially between 50 and 150m depths. Since IOSW characteristics are observed near 50m depth, on the southern part of this composite section, and PGW between 90 and 250m depths on its northern part, we conclude that this thermohaline gradient separates these two water masses. On the contrary, isopycnals are relatively flat except in the left hand part of the section (in the Gulf). Density values range between $\sigma_0 = 23$ and $26kg/m^3$, while values found in June 1992 lay between $\sigma_0 = 24$ and $28kg/m^3$ (Reynolds, ibid). These global density distributions are fairly similar to each other and rather different from winter density structures which show a steep and sharp density front near the Strait (see figure 4 of Brewer, 1978; figure 11 of Reynolds, 1993; figure 6 of Matsuyama et al., 1998). Surface temperature is slightly lower in the Strait (R12) than west (R13) and south of it (R11), an indication of enhanced mixing in the Strait. At this time of the year, the fresh water core

(IOSW) is rather a subsurface than a surface inflow, at least in the sampled area. Again we observe that PGW salinity near the bottom decreases from 40 psu in the Gulf to 38.5 psu at the head of the Gulf of Oman, showing that important dilution accompanies advection as discussed by Banse (1997) and Bower et al. (2000).

### 3.2 Short-term variability

During the GOGP99 cruise, sections R11, R12, R13 and R18 (see location on Figure 3) were repeated 3 times (October 10-13, October 21-23 and November 1-2) to evaluate the short-term variability of the hydrological features in this area. For sake of clarity, only the most informative figures are provided.

In the Gulf (section R13), salinity variations, from one realization to the following one, occur in both the upper and lower layers (not shown). In the lower layer (under 40m depth), the PGW core intensifies and widens between October 12 and 22, and decreases thereafter, indicating either a pulse of PGW water or an advection of salty water from the shallow UAE coastal region. During that month, surface salinity also increases in the southeastern part of the section while a fresh core disappears in the northwestern area. This evolution could be associated in part with the seasonal decrease of the IOSW inflow in the Gulf (Swift and Bower, 2003) or with lateral displacement of the IOSW core. Thermal features do not show significant changes between the three sections.

In the Strait (section R12), only the northern part of the section was sampled 3 times (not shown). Salinity decreases drastically (by more than 1 psu) in the bottom layer, which could indicate a short term trend or a lateral displacement of the PGW core. Indeed, in October-November, little seasonal variation of the PGW outflow was measured by Johns et al. (2003) near the Musandam Peninsula. Boundary of the inflowing IOSW core at 50 m depth shows opposite-sign displacements on the two-week periods, perhaps associated with a pulse.

Further south, R11 was sampled more completely over the three legs (see Figure 12). A striking aspect of the short-term variability is the major decrease of the PGW core with a thickness and width reduction by a factor 3 and a decrease in T and S maxima from $26^oC$ to $25^oC$ and from 39.5 to 38.5 psu respectively. We also note an increase in width of the IOSW core, as well as a decrease of its temperature and salinity. Section R18 also evidences a reduction of the PGW core between early October and beginning of November, and an increase in IOSW flux near the Iranian side of the section (not shown).

The global view deduced from these sections is a temporary increase of PGW in the Gulf, but a noticeable decrease of this water mass in and south of the Strait. This evolution can be explained by a pulse of warm and salty water from the coastal UAE area or from the source region of PGW, and a decrease of IOSW inflow in the Gulf. At the head of the Gulf of Oman, the observed features are compatible with an increased advection of IOSW from its source, shifting the PGW core laterally. Indeed, if the 0.5 psu, $1^oC$ decrease in the PGW core over one month (section R11) is compatible with ranges of seasonal changes, it seems too abrupt to be explained only by winter-summer differences.

## 4 Temporal variations of velocity and temperature from moorings and floats south of the Strait of Hormuz

South of the Strait of Hormuz, time series of velocity and temperature were obtained with an ADCP (D1) and two thermistor chains (T2, T3) from October 8 to November 9 1999 (see Figure 2). Two tide recorders were moored east and west of the Strait. Surface drifting buoys (Surdrift floats) drogued at 15 and 85m were released in and south of the Strait of Hormuz.

## 4.1 Velocity features

Alongshore and across-shore[5] velocity components were obtained from ADCP mooring D1. They have been processed to obtain high and low frequency components.

Complete records show an important tidal contribution to the horizontal flow component (Figure 13) as well as to vertical velocities (not shown). Across-shore flow (i.e. across-isobaths) is stronger than alongshore flow, with respective ranges of variations, $[-0.55, +0.45]m/s$ and $[-0.35, +0.35]m/s$. Vertical velocities range between $-0.04$ and $+0.04m/s$. Similar values have been obtained by Matsuyama (1994, 1998) with Doppler currentmeter recordings in the Gulf near the Strait of Hormuz. For both across-shore and alongshore flow, the barotropic part is intense and the baroclinic component reinforces surface currents. Furthermore, it is known that the spatial structure of tides near the Strait (not captured here by a single ADCP mooring) is complex.

Harmonic analysis of the time series of horizontal current reveals the existence of several semi-diurnal and diurnal components, M2, S2, K2, O1, K1 and P1, with associated peaks in the energy spectrum. Harmonic analysis of tide recorders measurements at the same location as D1 provides an amplitude ratio $\frac{A_{K1}+A_{O1}}{A_{M2}+A_{S2}} = 0.69$ characterizing a mixed tide (in the sense used by Defant, 1960).
Current ellipses for each of these major harmonics are plotted at several depths on Figure 14. Again they show across-shore alignment with dominant M2, K1 and S2 harmonics having $0.15, 0.10$ and $0.08m/s$ magnitude respectively. Vertical structure of horizontal currents indicate maximum amplitudes near the thermocline at 30m, most likely correlated with internal tides (see also hereafter), and a decrease toward the bottom, assumed to be associated with friction. Nevertheless, semi-diurnal component S2 and diurnal component K1 also show maxima near 90-100m depths, which can be associated with a secondary density gradient near the PGW core. On the contrary, Matsuyama (1994, 1998) and Johns and Olson (1998) find a predominance of K1 component in the barotropic tide west of the Musandam Peninsula; this reflects spatial variability of the tidal structure. Complexity also appears in the time variability of tidal currents: the onshore flow component exhibits a diurnal frequency around October 17, and a semidiurnal frequency around October 25 (see again Figure 13).

Low-pass filtered currents (at 25 hours) were then computed from ADCP mooring recordings. Residual currents exhibit substantial vertical and temporal variations (Figure 15). Current can locally reach $0.35m/s$ (near the surface), with mean velocity of $0.03m/s$, a value much lower than that ($0.2m/s$) found by Matsuyama (1998) and Johns et al. (2003) at a mooring located near strong bathymetric gradients, and assumed to lie in the PGW core. Mooring D1 did not record strong velocities below 100m depth, except a southward pulse of $0.10m/s$ between October 13 and 17; this pulse can be related to the episode of wide PGW core seen in the variability of section R18. The strong southward current near the surface (October 22-29) is related to a deepening of the thermocline by 10 to 15m, seen in thermistor chain T2 recordings (Figure 16). A northwesterly wind of $10m/s$ measured near mooring D1, by R/V D'Entrecasteaux on October 23, could account for this sudden change. In intermediate waters (depths of 35 to 63m), a dominant northward current is measured during the month of October, though with time variability; it corresponds to the IOSW inflow. These currents increase between beginning and end of October, in agreement with the short-term variability observed on sections R11 and R18.

## 4.2 Temperature variability

Temperature recordings at T2 and T3 reveal strong internal wave activity (Figure 16). Strong internal tides have already been observed in the vicinity of the Strait by Roe et al. (1997). Diurnal and semi-diurnal oscillations of isotherms are related to the barotropic tidal forcing described hereabove. Verti-

[5] these components are referenced to the local bathymetry, i.e. positive along-shore direction is northeastward ($60^o$ true) and positive onshore northwestward ($-30^o$ true)

cal displacements of these isotherms over a tidal cycle range between 5 and 20m. Maximum displacement is noted on T2 recordings, October 16.
These displacements can be computed using formula (6) in Pichon and Mazé (1990) for internal waves near shelf break. An estimate of their order of magnitude is related to the baroclinic component of velocity below the thermocline $u_2$ via

$$u_2 \;=\; c_0\eta/(H_2+\eta)$$

where $c_0^2 \;=\; g'H_1H_2/H(1-f^2/\omega^2)$ is the squared phase velocity of the internal wave, $H_1, H_2$ are mean thicknesses of the upper, lower layers (above or below the thermocline, $g'$ is reduced gravity, $f$ is the Coriolis parameter, $\omega$ is the wave pulsation, $\eta$ is the thermocline displacement due to the wave). Assuming $\eta << H_2$ (here $H_2 = 80m$), we obtain

$$\eta \;=\; H_2u_2/c_0$$

With $g' \;=\; 2.5\,10^{-2}m/s^2$, $H_1 \;=\; 30m$, $\omega \;=\; 2\pi/43200s^{-1}$, $f/\omega \;=\; sin(25^o)$, we have $c_0 = 0.74m/s$. Baroclinic tidal velocity is obtained by substracting a depth averaged velocity from the signal leading to $u_2 \sim \pm 0.1m/s$, whence $\eta \sim \pm 10m$.

Temperature recordings also reveal slower variability. At its time of largest width (near October 12) the PGW was recorded by mooring T2 (this cannot be clearly distinguished on Figure 16, but it is seen in data). Temperature recordings also indicate a cooling of the mixed layer and a deepening of the thermocline with time. This cooling is rather sudden on mooring T2 with a 15m deepening of the mixed layer, near October 19-20, while it is more continuous on mooring T3. This geographic difference of mixed layer evolution could originate in spatial variations of surface heating (or cooling) or in horizontal advection of cold surface water, or both.

To obtain more information on surface temperatures, we analyze the MCSST[6] maps provided by NAVOCEANO, at various dates around and during the GOGP99 experiment (see Figure 17). The K10 SST maps are composite images with 8.8 km spatial resolution.
First, it is interesting to compare the September 15 and October 15 maps. Noticeable cooling has occured on the whole Gulf between these two dates, while the Gulf of Oman undergoes surface warming with homogenization of temperature. Strikingly, the same evolution has occured between mid-september and mid-october 2000, 2001 and 2002 (not shown).
At the beginning of the period of interest (Oct. 15), a warm surface region (with temperature $30^oC$) extends from the Strait eastward to $57^o30'E$ north of $25^oN$; a colder patch (with temperature $29^oC$) lies along the Iranian coast, east of $59^oE$. The following image (Oct. 22) shows that this colder patch has not evolved substantially, but the warm region has retreated to $57^oE$ north of $25^oN$, a variation compatible with the decrease in temperature measured by mooring T2 but not by T3. On October 30, the $30^oC$ isotherm has moved northward into the Strait; this is related to the decrease in temperature measured then by mooring T3. Also, the colder patch (at $29^oC$) has considerably extended near the Iranian coast, and has formed a separate blob between $57^o45'E$ and $59^o15'E$. This blob, possibly associated with local upwelling, could be related to the increase in IOSW observed in the 3 realizations of hydrological sections R11 and R18. More information on this upwelling is given in Part 2 of the paper.
To conclude on thermal variations, atmospheric fluxes and their spatial inhomogeneity certainly play an important role in the evolution of surface temperatures : the strong winds measured by R/V D'Entrecasteaux can induce a deepening and a cooling of the mixed layer. But, since moorings T2 and T3 are only 30km apart, the different variations of their surface temperatures cannot be accounted for by large-scale atmospheric fluxes. Such fluxes must be local. Southeastward winds, such as those measured mi-October south of the Strait, can favor the development of an upwelling region near the Iranian coast. Nevertheless, advection certainly plays a role: part 2 will show that a cyclonic general circulation occupies most of the Gulf of Oman. Such currents can advect cold water lying initially near the Iranian coast, closer to the Strait, as observed in the MCSST

[6]Multi Channel Sea Surface Temperature

maps.

### 4.3 Surdrift float trajectories

Five surface floats, drogued at 15 or 85m, and positionned via GPS, were released and followed trajectories in the vicinity of the Strait. Three-day filtering of velocity magnitudes eliminated oscillations at the tidal and inertial periods, but retained variability on periods characteristic of changes in atmospheric conditions (see hereafter). These trajectories are represented on Figure 18. The release positions and lifetime are specified in table 3. Buoys drogued at 15m lie above IOSW and mostly followed mixed layer motions, while buoys drogued at 85m could follow the PGW core in the Strait.

Buoys 14677 and 14766 were both drogued at 15m and released at close locations (3km but 4 days apart). Buoy 14677, launched on October 8, followed a northward route along the coast of Oman for a week, before veering south along the Iranian coast, and coming back near its initial position after 12 days. Though few wind data (mostly obtained from ships) are available near the Strait at that period, the wind measured in the southeastern part of the Strait near October 8-10 was northwestward, and it turned southeastward on October 16. Later, this float entered the northern part of the Gulf of Oman and was caught in a small anticyclonic eddy, looping with 12 km radius and 5 day period, near isobath 200m (close to $25^o30'N - 56^o55'E$). It was ejected after one loop and its final trajectory was northward (a northward wind was measured on November 1,2 in the southern part of the Strait). The mean velocity of buoy 14677 was close to $0.2m/s$.
On the contrary, buoy 14766 (which lived only for 10 days) had a fairly moderate displacement, noticeably influenced by tidal motions. Launched on October 12 (with northwestward wind conditions measured on the 8-10), it turned southeast close to the 16 (with southeastward wind). Finally, it followed a short northeastward route also along the coast of Oman (a northward wind was measured on October 22, south of this location). It was unfortunately trawled on October 22. Its mean velocity over its lifetime was $0.15m/s$.

Buoy 14916, also drogued at 15m, and launched on October 9, headed northwestward initially (like buoy 14677), showed a reversal in trajectory after a week, going southeastward for another 4 days and finally northward again before being trawled. Its trajectory remained in the near vicinity of the Iranian coast. This buoy displayed weaker motion than the previous two, with mean velocity of only $0.09m/s$, perhaps due to the proximity of the coast (and thus to partial shielding from the wind).

Buoys 14745 and 14979, both drogued at 85m, had mean velocity between 0.05 and $0.12m/s$. Buoy 14745 lived only for 10 days (before being trawled) and exhibited notable tidal oscillations along the Strait axis. Its initial trajectory was northeastward, into the deep trough which contains the PGW core. Its final displacement was northward with lateral oscillations. Buoy 14979 did not display substantial displacement for the first week before heading south(-east) and being caught in an anticyclonic eddy slightly south of that of buoy 14677. The loop performed by buoy 14979 in that eddy had 15km radius and 5 day period, comparable with those of buoy 14677. The possible nature and origin of this eddy will be discussed in part 2 of the paper in relation with other data.

## 5 Discussion and conclusions

Data analysis of GOGP99 experiment has clearly shown the outflow of PGW lying on the Omani slope and the inflow of IOSW at the entrance of the Strait of Hormuz. The hydrological structure in the Gulf and in the Strait is composed (most often) of a 30m thick mixed layer overlying a stratified water column containing the PGW core, while at the head of the Gulf of Oman, the fresher and colder IOSW core is clearly seen above and next to the PGW outflow. Most of this IOSW core has been missed on sections R12 and R13 which do not extend close enough to the Iranian coast, though a trace of IOSW is observed in the Gulf on the northwestern tip of

section R13. Using a composite section following the PGW maxima along the Strait axis, a thermohaline gradient appears between PGW and IOSW at the head of the Gulf of Oman. But this thermohaline gradient is not associated with a sharp density front as was observed in winter. Hydrological sections also characterize the PGW core evolution along the Strait of Hormuz, with temperature and salinity decreasing downstream by $3^oC$ and 1.5 psu over 150 km, most likely by reason of mixing with the fresher IOSW core.

Geostrophic velocities were computed on section R13, using previous data from an ADCP morring nearby. A level of reference of 30m was used at which a mean flow was computed. The resulting velocity section shows a deep outflow with velocity slightly less that 0.4 m/s, but also a weaker deep inflow and a surface inflow along the Omani coast, the realism of which has to be proven. Transports for inflows and outflows above and below 45m depth were found similar to those computed by Johns et al. (2003), and relatively independent of the level of reference, or of the realization of the section. Nevertheless, direct measurements of velocity at mooring D1, south of the strait, show the complexity and variability of the velocity structure and suggest strong caution with geostrophic velocity interpretation.

Over a one month period, noticeable changes in the hydrological structure in the vicinity of the Strait have been observed, and exhibited opposite trends in and out of the Gulf. In the Gulf, a noticeable temporary increase of salinity was associated with reduction of IOSW inflow and perhaps local advection of salty water. In the Strait and in the Gulf of Oman, IOSW inflow seemed to increase and to squeeze the PGW outflow and displace it sideways. In particular, the reduction of PGW lateral extent with time on section R11 is correlated with the wider IOSW core. In the Gulf of Oman, the temperature and salinity decrease in the mixed layer can also be associated with strong wind events and/or advection of cooler water. ADCP measurements and float 14916 trajectory show reversals of currents in the upper layer over 4-7 day periods after October 15. Such flow reversals can be associated with changes in wind direction, which can also induce upwelling near Ra's Jagin (Iranian coast). Such an upwelling, or advection of cold water along the Iranian coast, could in turn enhance the flux of cold and fresh water associated with the stronger IOSW flow.

ADCP and moored thermistor data indicate that high-frequency variability is dominated by semi-diurnal M2 and S2 and diurnal K1 components of tide with complex vertical structures. Tides exhibit maximum amplitude near the surface pycnocline; this notable signal is associated with internal waves. A simple calculation showed that the amplitudes of these internal waves could be estimated from the baroclinic velocities of the tidal current. A secondary maximum of tidal currents (S2 and K1) at roughly 100m depth can be related to the interface between IOSW and PGW. Deepening of the mixed layer occurs more rapidly at one of the two thermistor chain moorings; this may be due to atmospheric cooling or wind bursts of limited extent or to the advection of colder water from a neighboring source (such as a local upwelling).

At subtidal time scale, mooring recordings southward flow below 100m depth near Oct.17 (i.e. between the first and second hydrological surveys). Currents in the 40-65m layer are mostly northward, compatible with maximum inflow of IOSW near October 31st. The low-frequency residual currents are weaker than previous model output (by a factor 2, see Bower et al., 2000). This may be due to the location of the ADCP mooring. These velocity measurements show important variability of the currents, both in amplitude and in the vertical structure which evolves from baroclinic (e.g. October 17) to nearly barotropic (October 31). These velocity and temperature time-series confirm the water mass variability observed in the repeated hydrological sections with decreasing PGW and increasing IOSW fluxes. They also indicate short term surface current variability (with intense southward currents from October 23 to 26), compatible with buoy 14677 trajectory.

Composite maps of surface temperature indicate the continuous retreat of warm water northward from the Omani coast between mid and end of October, and the more sudden progression of colder water along the Iranian coast after Oct. 22 (Figure 17). These elements are compatible with the observations of thermistor chain moorings and between the various realizations of hydrological sections R11 and R18.

Surface buoys drogued at 15 or 85m had lifetimes between 2 and 4 weeks. In that short lifespan, they indicated short-term surface current reversal, related to changes in wind direction (such changes are common in the region, as for instance the Shamal-Shakki (or Kaus) alternation at the passage of atmospheric fronts; see Reynolds, 1993). Trajectory of buoy 14916 drogued at 15m, with reversals in direction over a 4 to 7-day period, shows considerable acceleration near October 16; this acceleration is consistent with local wind bursts which also induce a deepening of the mixed layer measured at mooring T2. At the head of the Gulf of Oman, buoys 14677 and 14979 drogued at 15 and 85m indicate the presence of a small anticyclone the generation of which will be analyzed in Part 2.

Obviously, this dataset though large, is not extensive enough to allow firm conclusions on all aspects of this work. Most notable are the following shortcomings:

- hydrological sections in the Strait were cut short in the Iranian waters, and did not allow accurate sampling of the IOSW core at that location;
- a second ADCP mooring did not work so that the maximum velocities of the PGW and IOSW inflow were not measured;
- atmospheric data is not available at high resolution to confirm short-scale wind or heat fluxes variability;
- many surdrift buoys were trawled after two to four weeks.

These shortcomings suggest future measurements which could include

- releasing buoys with 40 to 60m deep drogues in the northern part of the Gulf of Oman to follow the IOSW;
- repeated seeding of the PGW outflow with buoys with 150m drogue or with Rafos floats near the head of the Gulf of Oman to help quantify the occurence of small eddies there;
- installing currentmeter moorings and thermistor chains on the pathway of PGW in the Gulf and of IOSW in the Gulf of Oman to provide upstream conditions for the observed variability in the Strait of Hormuz...

Considering the cost of in-situ measurements, high-resolution numerical models could also be of use to help discriminate between several mechanisms for the observed variations of the flow and for the formation of eddies.

### acknowledgments

We gratefully acknowledge the help of the Naval Oceanographic Office (USA) which kindly provided the K10 SST images. Thanks are due to Y Camus (SHOM/CMO) for his participation in the design of this experiment, and to Captains and Crews of R/V D'Entrecasteaux and Laplace for data collection; EPSHOM/CMO/CM engineers and technicians did a substantial part of data processing. This work is a contribution to the GOGP99 experiment and to S. Pous PhD thesis.

## References

[1] Ahmad F. and S.A.R. Sultan, Annual mean surface heat fluxes in the Arabian Gulf and the net heat transport through the Strait of Hormuz", *Atmosphere-Ocean*, 29, 54-61, 1990.

[2] Banse K., Irregular flow of Persian(Arabian) Gulf water to the Arabian Sea, *J. Mar. Res.*, 55(6), 1049-1067, 1997.

[3] Bower A.S., H.D. Hunt and J.F. Price, Character and dynamics of the Red Sea and Persian Gulf outflows, *J. Geophys. Res.*, 105(C3), 6387-6414, 2000.

[4] Brewer P.G. and D. Dyrssen, Chemical oceanography data from the Persian Gulf and Gulf of Oman, *Progress in Oceanography*, 14, 41-55, 1985.

[5] Defant A., Volume 2 of Physical Oceanography, Pergamon Press, 1960.

[6] Chao S.Y., T.W. Kao and K.R. Al-Hajri, A numerical investigation of circulation in the Arabian Gulf, *J. Geophys. Res.*, 97(C7), 11.219-11.236, 1992.

[7] Hartmann M., H. Lange, E. Seibold and E. Walger, Oberflachensedimente im Persischen Golf und Golf von Oman, *Meteor Forsch. Ergebn.*, 4, 1-76, 1971.

[8] Johns W.E. and D.B. Olson, Observations of Seasonal Exchange through the Strait of Hormuz, *Oceanography*, 11, 58, 1998.

[9] Johns W.E., F. Yao, D.B. Olson, S.A. Josey, J.P. Grist and D.A. Smeed, Observations of seasonal exchange through the Straits of Hormuz and the inferred heat and freshwater budgets of the Persian Gulf. *J. Geophys. Res.*, 108, C12, 3391, doi:10.1029/2003JC001881, 2003.

[10] Matsuyama M., T. Senjyu, T. Ishimaru, Y. Kitade, Y. Koike, A. Kitazawa, T. Miyazaki and H. Hamada, Density front in the Strait of Hormuz, J. Tokyo Univ. Fischeries, 81, 85-92, 1994.

[11] Matsuyama M., Y. Kitade, T. Senjyu, Y. Koike and T. Ishimaru, Vertical structure of a current and density front in the Strait of Hormuz, in it Offshore Environment of the ROPME Sea Area after the war-related oil spill, edited by A. Otsuki, M.Y. Abdulraheem and R.M. Reynolds, Terra Sci. Publ. Co., Tokyo, 23-34, 1998.

[12] Meshal A.M. and H.M. Hassan, Evaporation from the coastal waters of the central part of the Gulf, *Arab J. Sci. Res.*, 4, 649-655, 1986.

[13] Pichon A. and R. Mazé, Internal tides over a shelf break: analytical models and observations. *J. Phys. Oceanogr.,*, 20 (5), 657-671, 1990.

[14] Privett D.W., Monthly charts of evaporation from the North Indian Ocean, including the Red Sea and the Persian Gulf, *Q. J. R. Meteorol. Soc.*, 85, 424-428, 1959.

[15] Reynolds R.M., Physical Oceanography of the Gulf, Strait of Hormuz, and the Gulf of Oman-Results from the Mt Mitchell Expedition, *Mar Pollution Bull.*, 27, 35-59, 1993.

[16] Roe H.S. J. et al., RRS Charles Darwin Cruise 104 Leg 1, 12 Feb - 19 Mar 1997. Scheherezade: an interdisciplinary study of the Gulf of Oman, Strait of Hormuz and the southern Arabian Gulf, *Southampton Oceanography Centre, Cruise Report No. 9*, 77 pp, 1997.

[17] Schlitzer R., Ocean Data View, http:\\www.awi-bremerhaven.de/GEO/ODV, 2003.

[18] Smith W.H.F. and D.T. Sandwell, Global Sea Floor Topography from Satellite Altimetry and Ship Depth Soundings, *Science Magazine*, vol. 277, issue 5334, 1997.

[19] Sultan S.A.R. and N.M. Elghribi, Temperature inversion in the Arabian Gulf and the Gulf of Oman, *Continental Shelf Res.*, 16(12), 1521-1544, 1996.

[20] Swift S.A. and A.S. Bower, Formation and circulation of dense water in the Persian Gulf, *J. Geophys. Res.*, 108(C1), 2003. doi:10.1029/2002JC001360.

Table 1: Physical oceanography measurements taken during the GOGP1999 cruise

| Section Name | Number of profiles | Data Type | Start Date | End Date |
|---|---|---|---|---|
| | | *Strait of Hormuz Sections* | | |
| R13a | 4 | CTD | Oct. 11, 1999 13h35 | Oct. 11, 1999 17h38 |
| R12a | 4 | CTD | Oct. 12, 1999 11h50 | Oct. 12, 1999 13h51 |
| R11a | 6 | CTD | Oct. 12, 1999 17h39 | Oct. 12, 1999 22h06 |
| R18a | 14 | CTD, XBT, XCTD | Oct. 13, 1999 02h01 | Oct. 13, 1999 10h11 |
| R13b | 8 | CTD | Oct. 22, 1999 04h07 | Oct. 22, 1999 10h07 |
| R12b | 4 | CTD | Oct. 22, 1999 15h11 | Oct. 22, 1999 17h44 |
| R11b | 10 | CTD | Oct. 22, 1999 21h23 | Oct. 23, 1999 02h31 |
| R18b | 10 | CTD | Oct. 23, 1999 05h44 | Oct. 23, 1999 11h33 |
| R18c | 9 | CTD | Nov. 01, 1999 08h40 | Nov. 01, 1999 13h58 |
| R19 | 5 | CTD | Nov. 01, 1999 16h31 | Nov. 01, 1999 19h07 |
| R11c | 7 | CTD | Nov. 01, 1999 20h39 | Nov. 01, 1999 23h39 |
| R12c | 10 | CTD | Nov. 02, 1999 05h11 | Nov. 02, 1999 09h12 |
| R13c | 8 | CTD | Nov. 02, 1999 13h30 | Nov. 02, 1999 18h35 |

Table 2: Mooring measurements taken during the GOGP1999 cruise

| Mooring Name | Profil type | depth range | Lat/Lon | Start Date | End Date |
|---|---|---|---|---|---|
| D1 | Velocity | 23-115 m | $25^o$36.1N/$57^o$00.5E | Oct. 08, 1999 | Nov. 08, 1999 |
| T2 | Temperature | 03-83 m | $25^o$36.2N/$57^o$00.1E | Oct. 09, 1999 | Nov. 08, 1999 |
| T3 | Temperature | 03-83 m | $25^o$24.0N/$56^o$42.9E | Oct. 09, 1999 | Nov. 08, 1999 |

Table 3: Surdrift drifters deployed during the GOGP1999 cruise

| Buoy Name | Drogue Depth | Deployment | | | End Date | T | ΔL | V |
|---|---|---|---|---|---|---|---|---|
| | | Start Date | Lat | Lon | | | | |
| 14677 | 15 m | Oct. 08, 1999 | $25^o$59.94N | $56^o$54.24E | Nov. 06, 1999 | 30 | 679 | 20 |
| 14745 | 85 m | Oct. 12, 1999 | $26^o$16.98N | $56^o$07.98E | Oct. 22, 1999 | 10 | 129 | 05 |
| 14766 | 15 m | Oct. 12, 1999 | $25^o$59.94N | $56^o$55.98E | Oct. 22, 1999 | 10 | 196 | 15 |
| 14916 | 15 m | Oct. 09, 1999 | $25^o$37.38N | $57^o$10.74E | Oct. 23, 1999 | 15 | 177 | 09 |
| 14979 | 85 m | Oct. 17, 1999 | $25^o$55.26N | $56^o$31.68E | Nov. 08, 1999 | 23 | 304 | 12 |

[7]T is the total operating time (day). ΔL = total displacement (km). V = Mean scalar speed (cm $s^{-1}$) of the low-pass filtered (at three days) Surdrift trajectories.

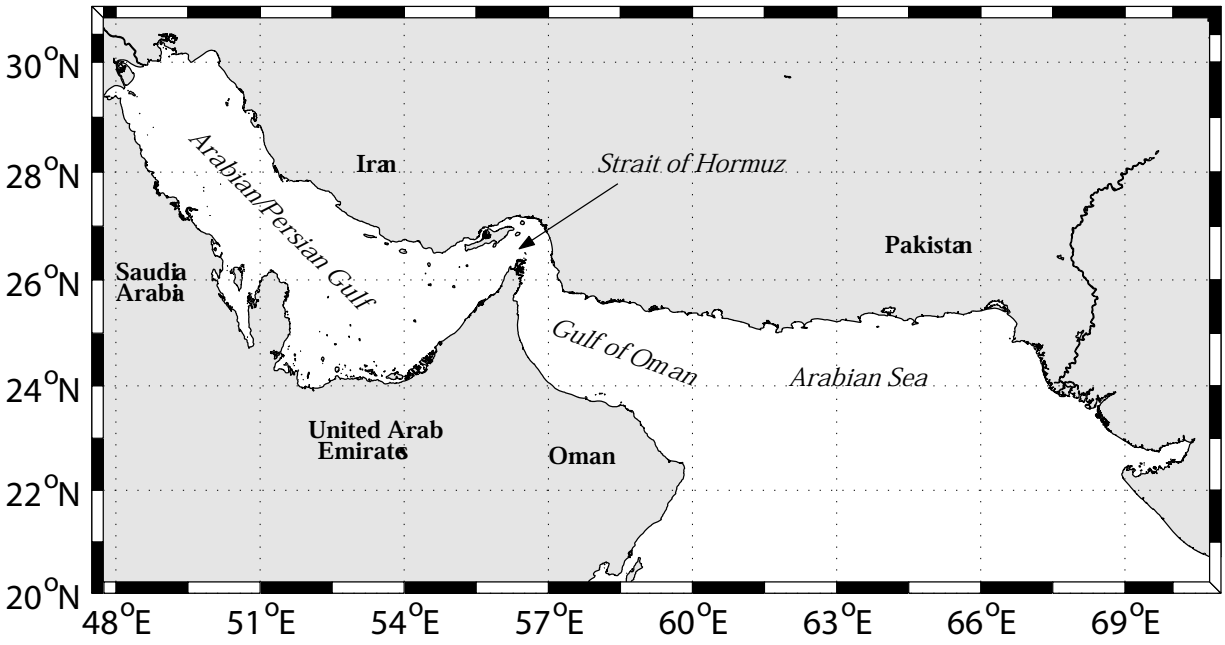


Figure 1: Chart of the Arabian/Persian Gulf, Strait of Hormuz and Gulf of Oman.

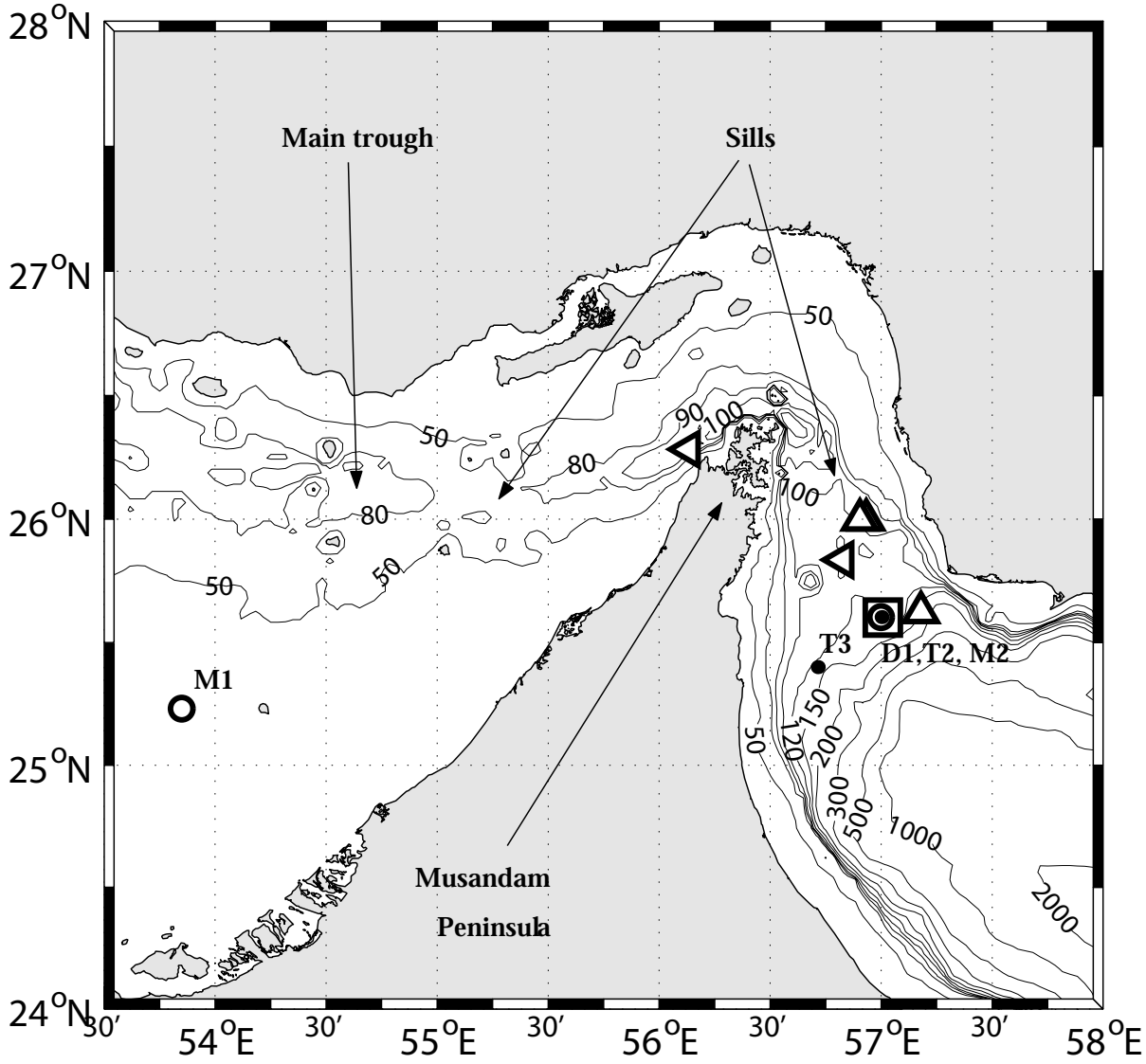


Figure 2: Bathymetry of the Strait of Hormuz and the Gulf of Oman from Etopo2 (Smith et al., 1997). Mooring sites and drifting buoy deployements are indicated : dots for temperature recorders moorings T2 and T3, circles for tide recorders M1 and M2, squares for ADCP mooring D1, triangles for initial deployement of drifters. Triangle orientations indicate drogues depth: 15 m (up) and 85 m (left).

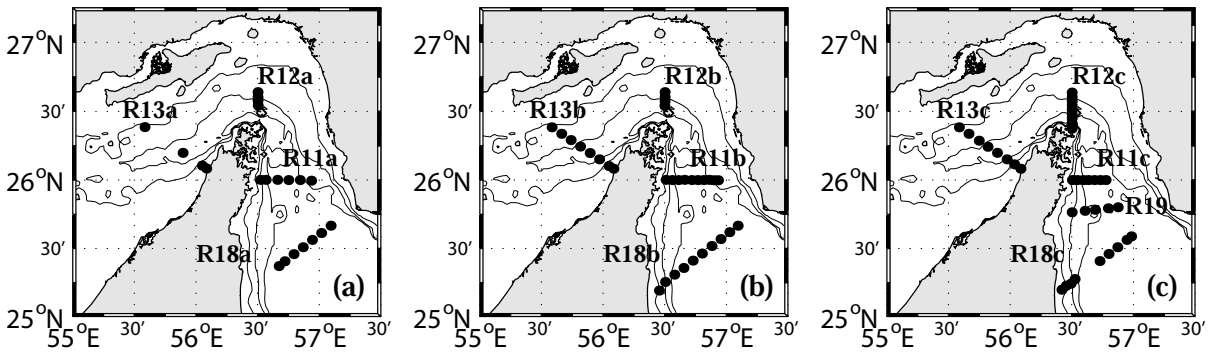


Figure 3: CTD stations in the vicinity of the Strait of Hormuz for the three legs: October, 11-13 1999 (a), October, 22-23 1999 (b) and November, 1-2 1999 (c). 50, 80 and 100 m isobaths from Etopo2.

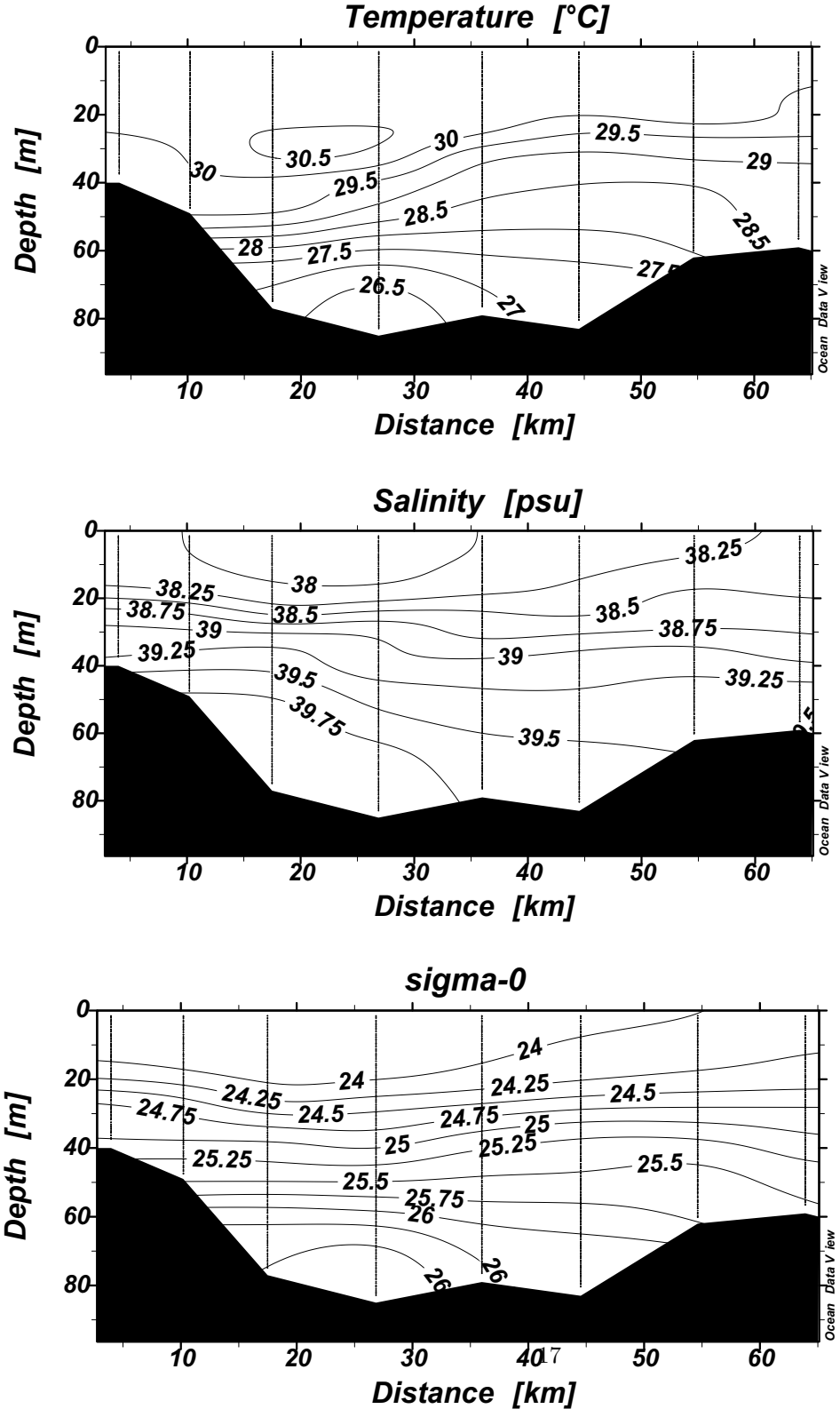


Figure 4: Cross-section R13c in the Arabian/Persian Gulf (location in Figure 3c) performed on November 2 1999. Temperature, salinity and potential density sections. Vertical lines indicate cast positions.

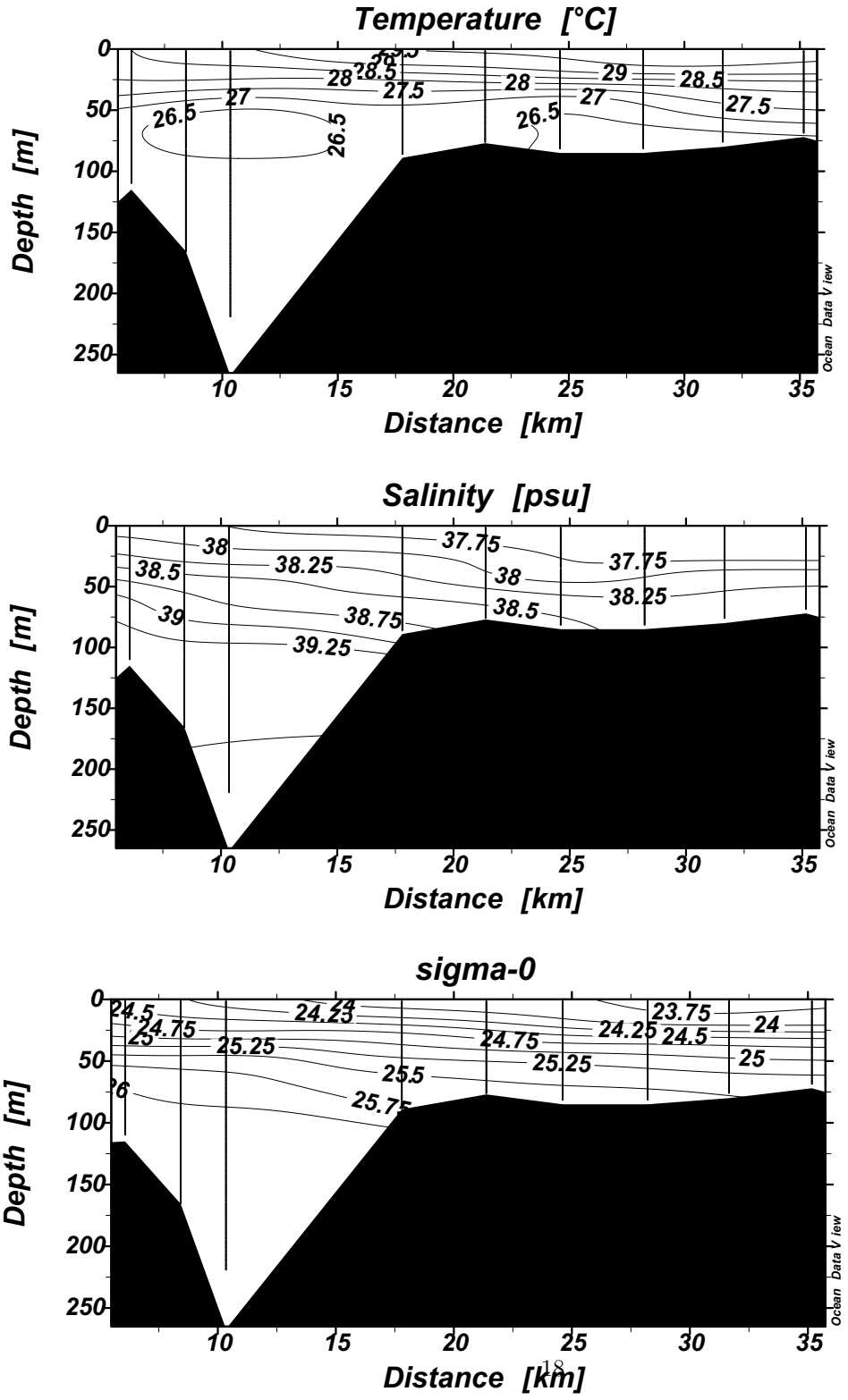




Figure 5: Meridional section R12c in the Strait of Hormuz (location in Figure 3c) performed on November 2 1999. Temperature, salinity and potential density sections. Vertical lines indicate cast positions.

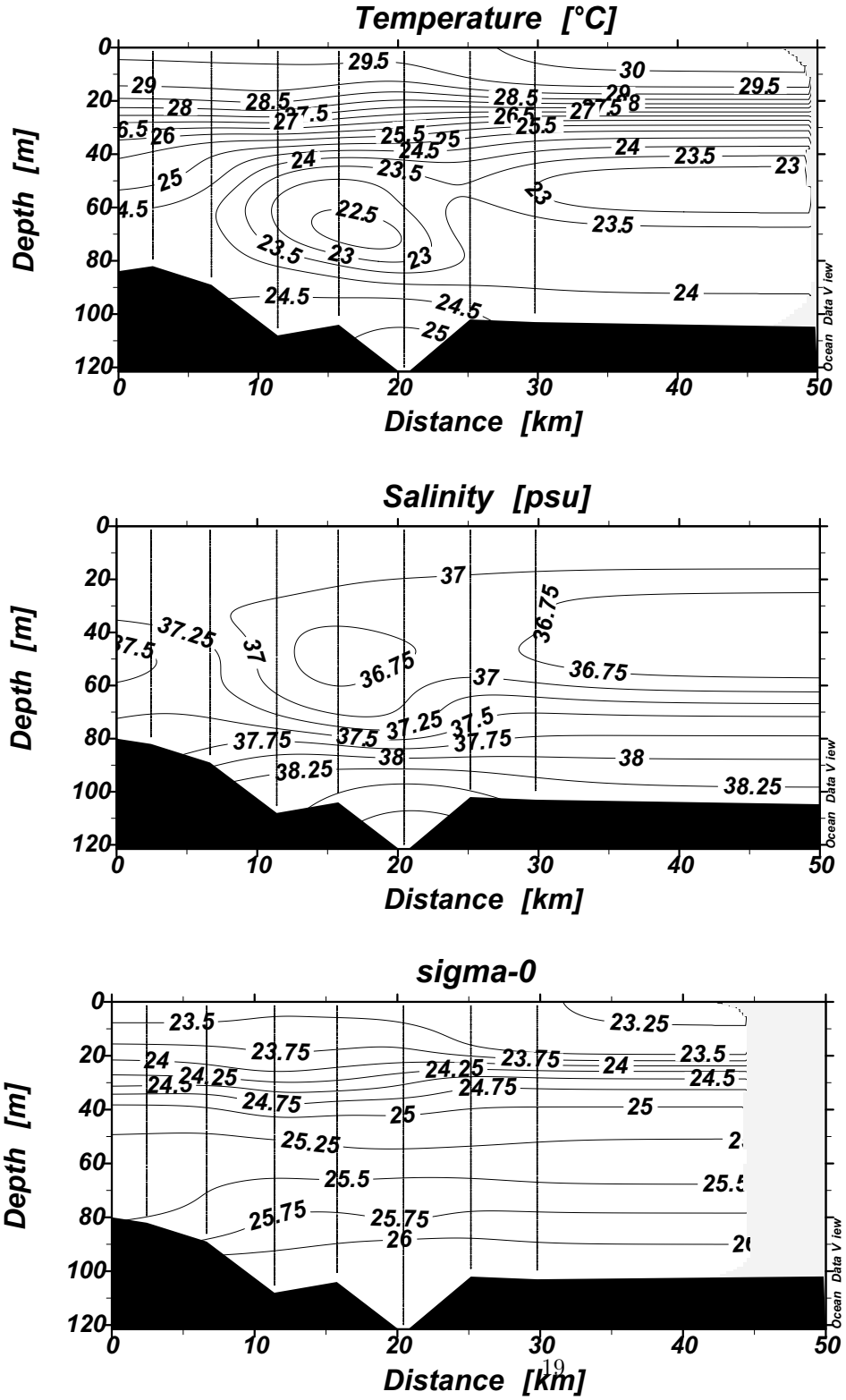




Figure 6: Zonal section R11c in the Gulf of Oman (location in Figure 3c) performed on November 1 1999. Temperature, salinity and potential density sections. Vertical lines indicate cast positions.

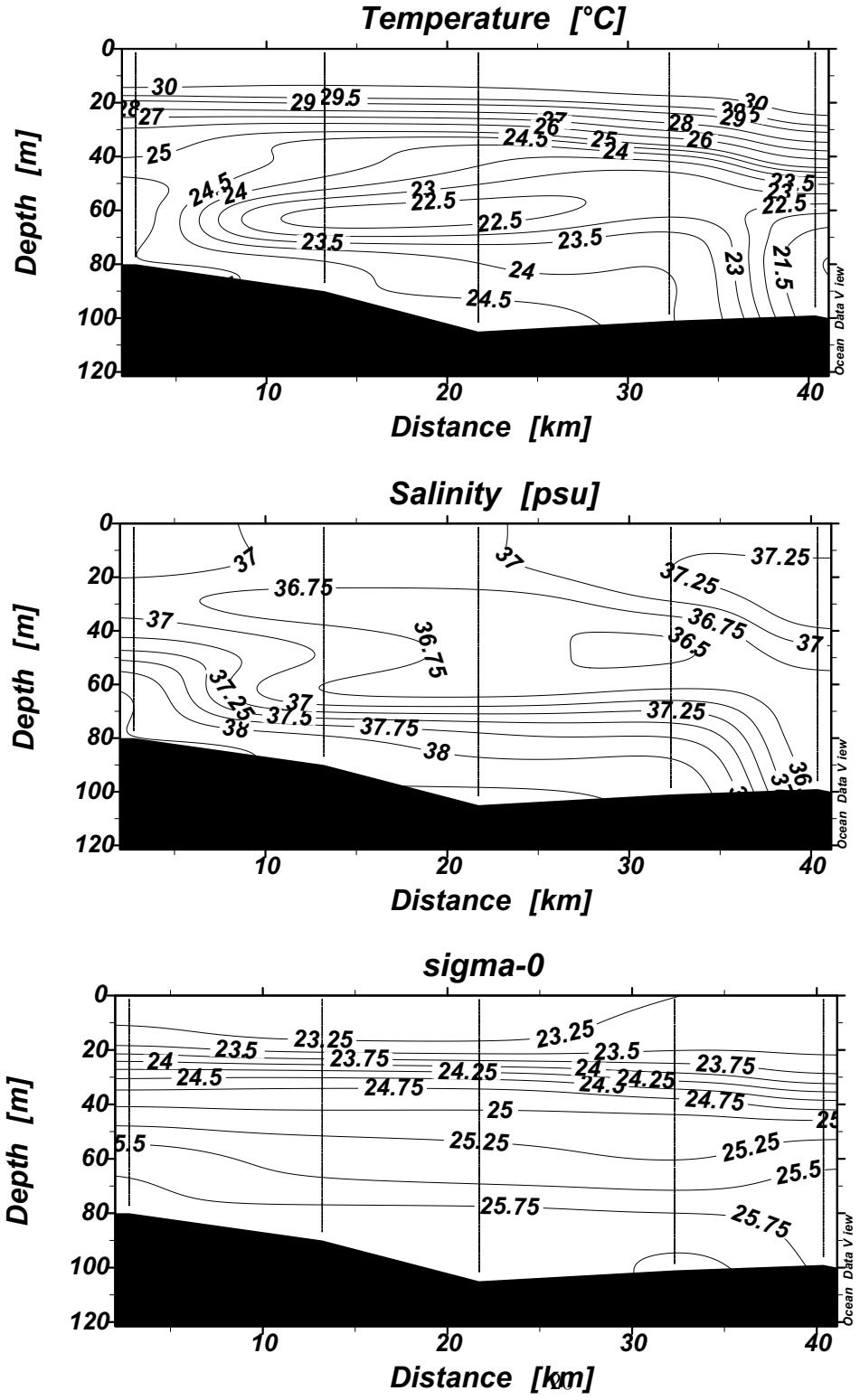


Figure 7: Zonal section R19 in the Gulf of Oman (location in Figure 3c) performed on November 1 1999. Temperature, salinity and potential density sections. Vertical lines indicate cast positions.

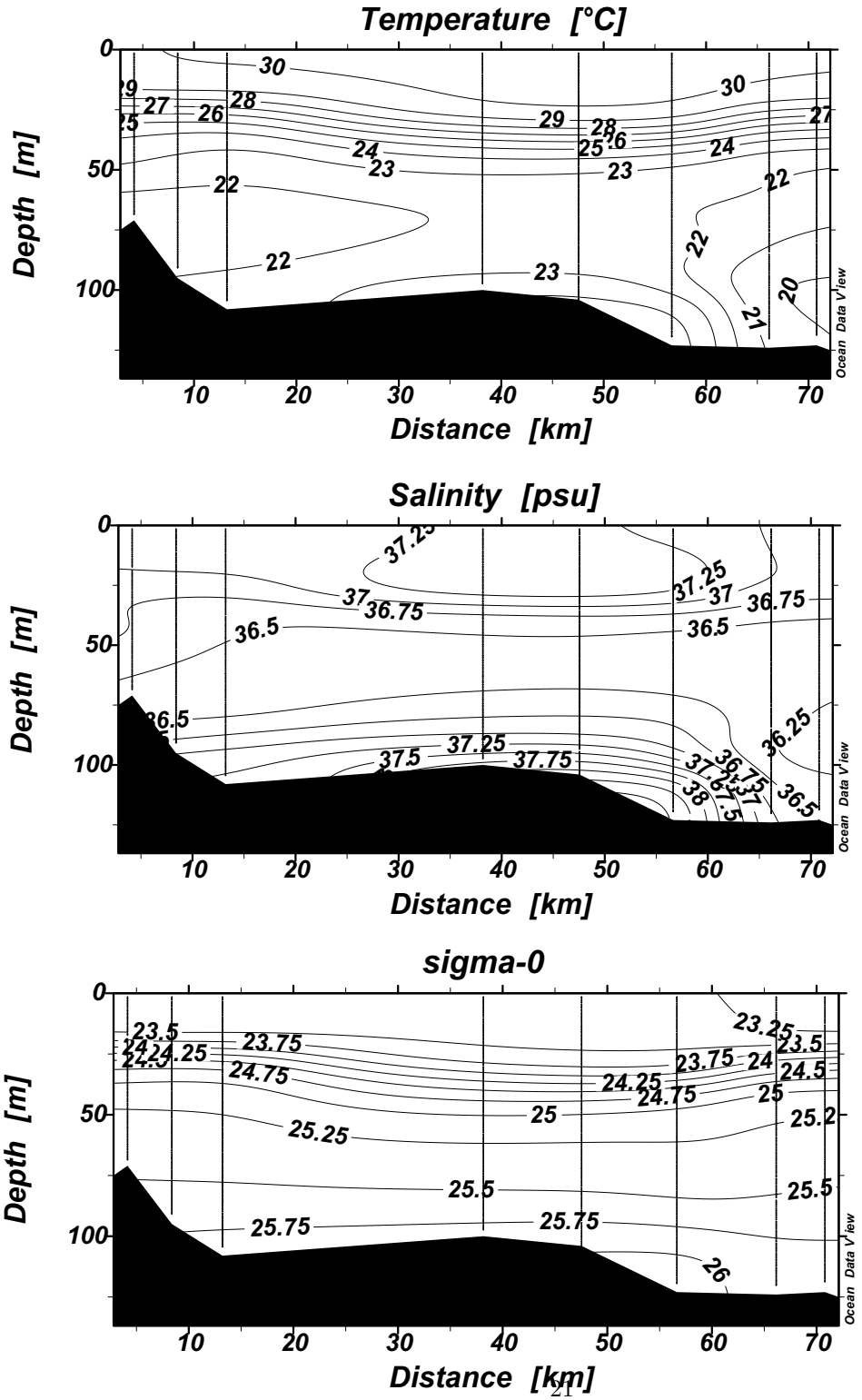




Figure 8: Zonal section R18c in the Gulf of Oman (location in Figure 3c) performed on November 1 1999. Temperature, salinity and potential density sections. Vertical lines indicate cast positions.

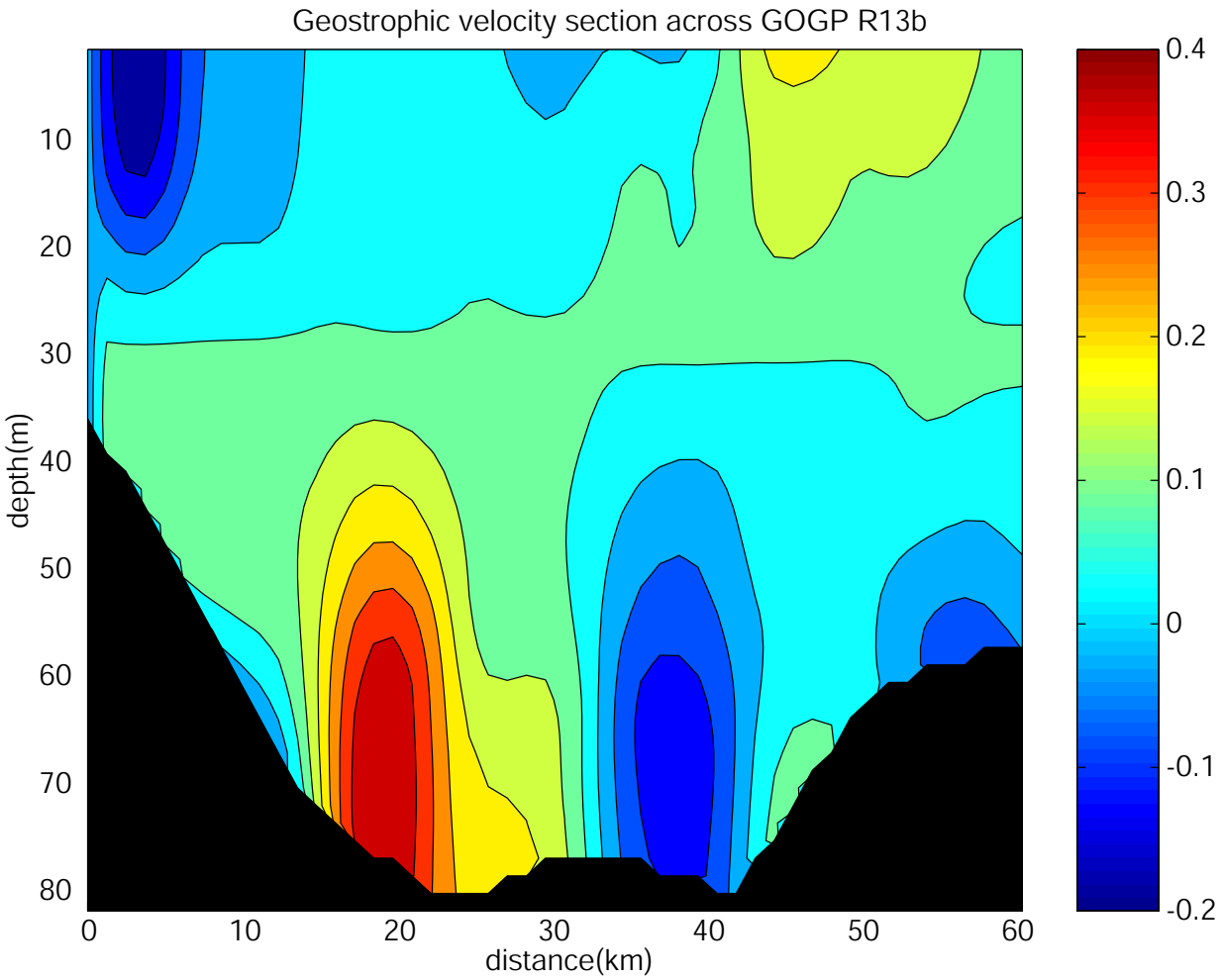


Figure 9: Geostrophic velocity computed on section R13b with a reference level at 30m (a mean flow of 0.09 m/s was added).

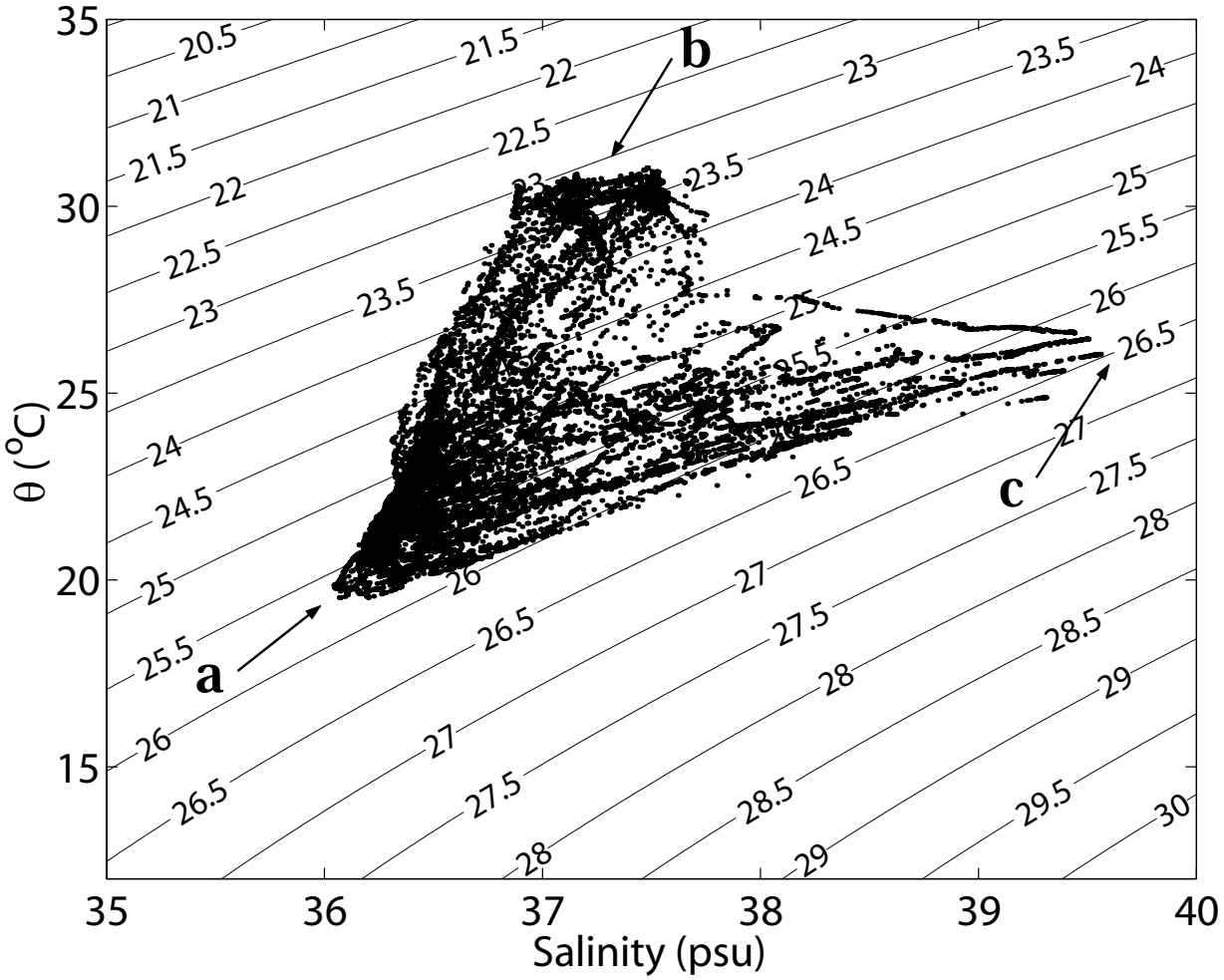


Figure 10: T-S diagram from hydrological data of sections R11, R19 and R18 between October 11 and November 2 1999. The 3 characteristic water masses in the southern part of the Strait of Hormuz are indicated: IOSW (a), mixed surface water (b) and PGW (c).

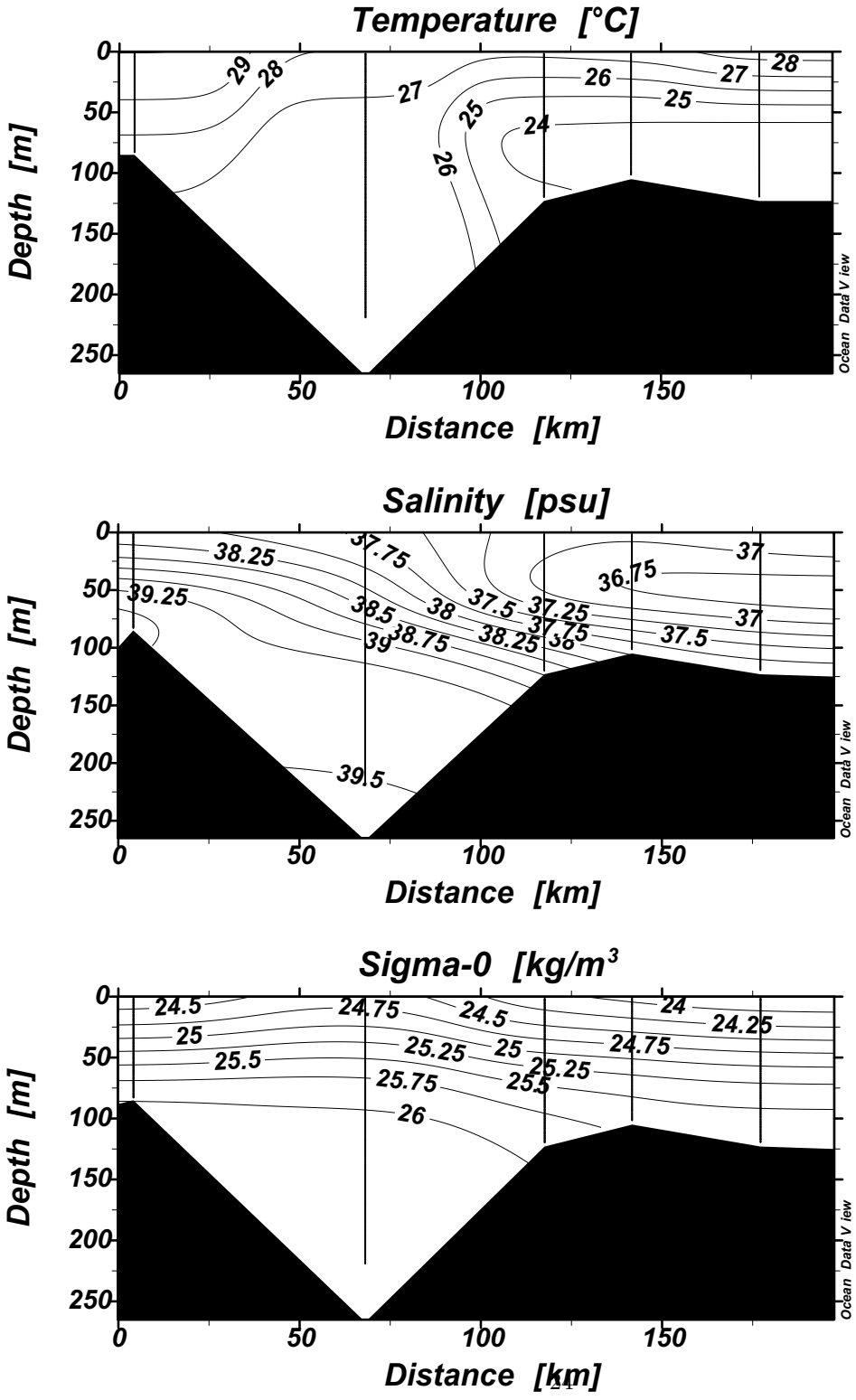


Figure 11: Composite section along the axis of the channel following the most undiluted PGW, from data of R13c, R12c, R11c, R19 and R18c sections performed on November 1-2 1999. Temperature, salinity and potential density sections. Vertical lines indicate cast positions.

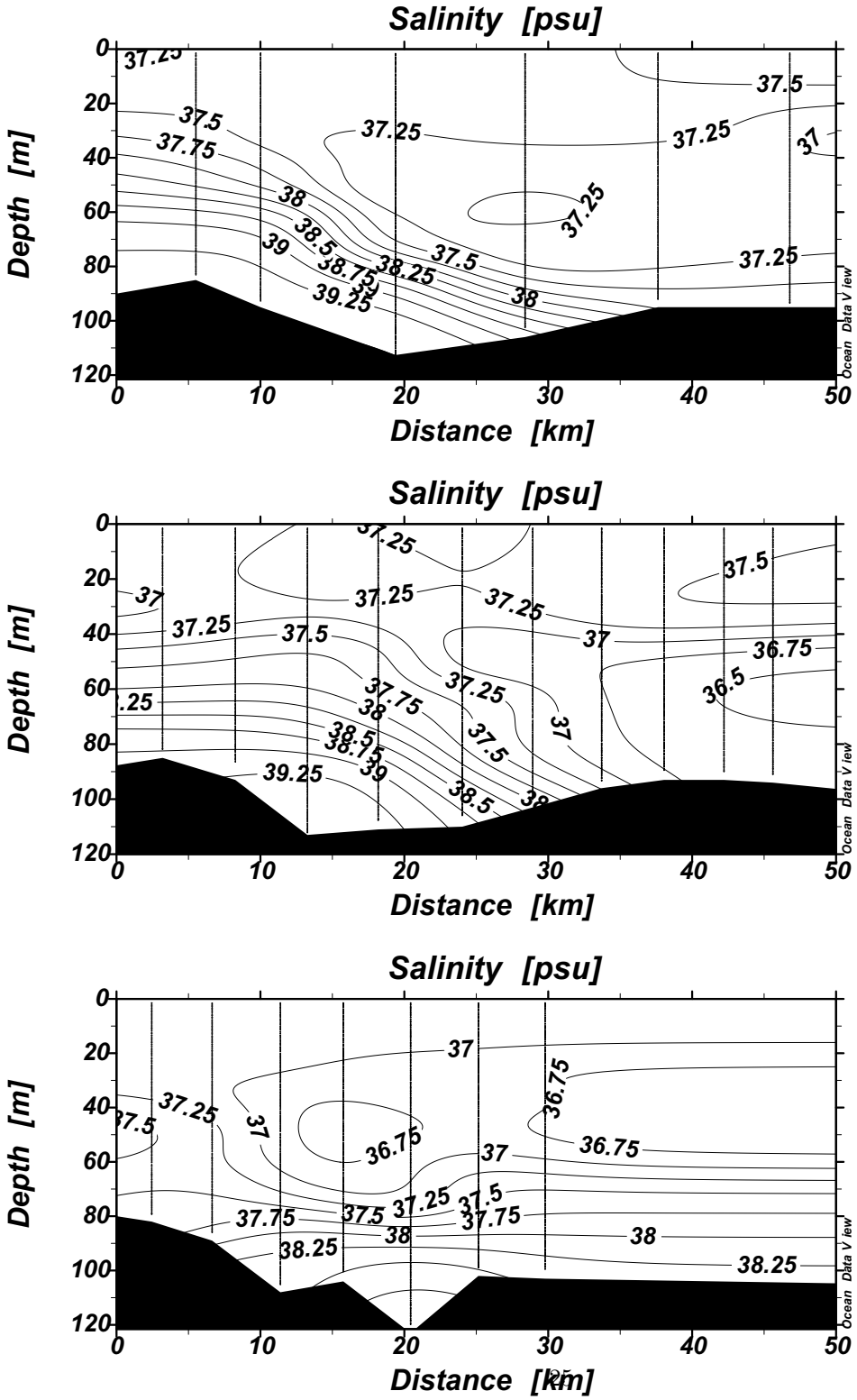


Figure 12: Repeated salinity section R11 in October 1-11, October 21-22 and November 1-2 1999. Vertical lines indicate cast positions.

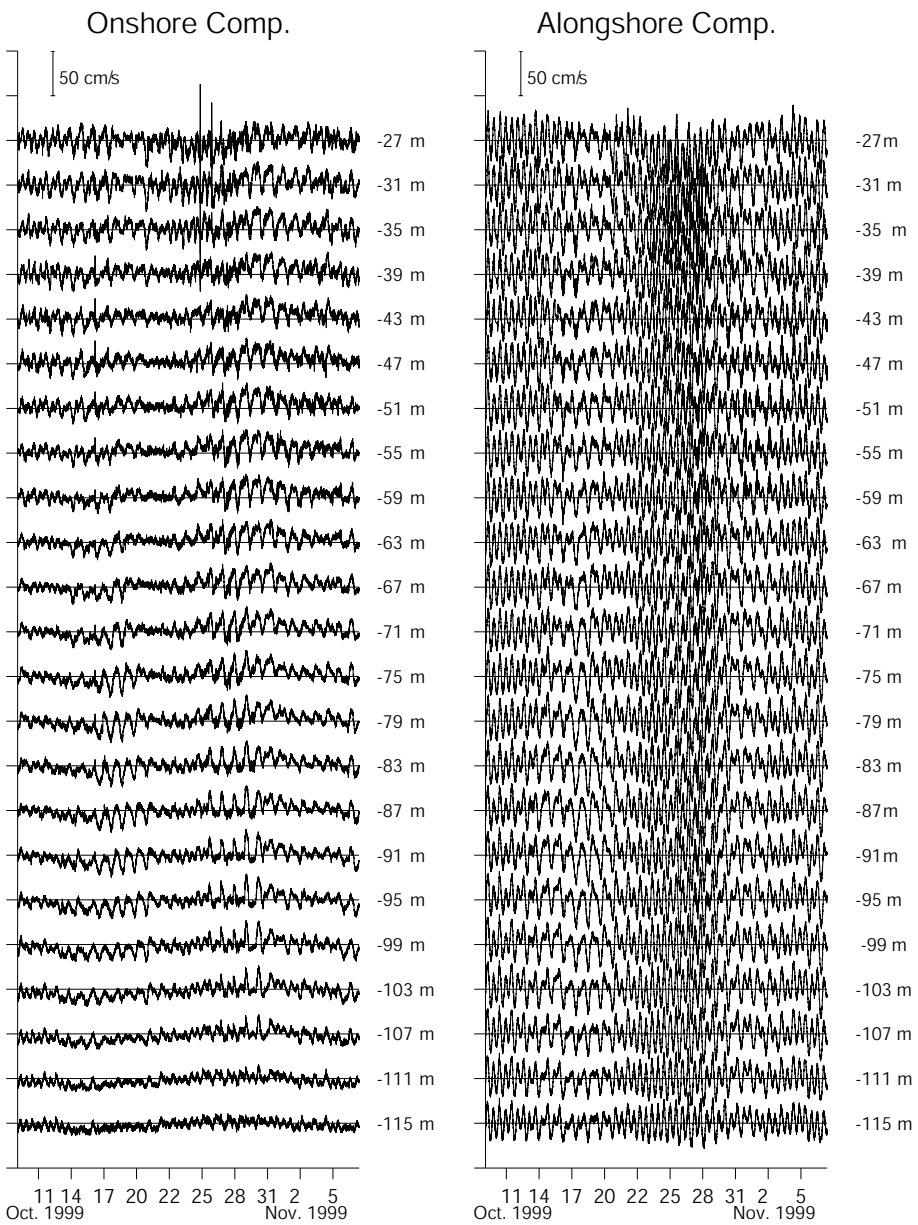


Figure 13: Time series of onshore and alongshore components of velocity at mooring D1, with 4 m vertical spacing.

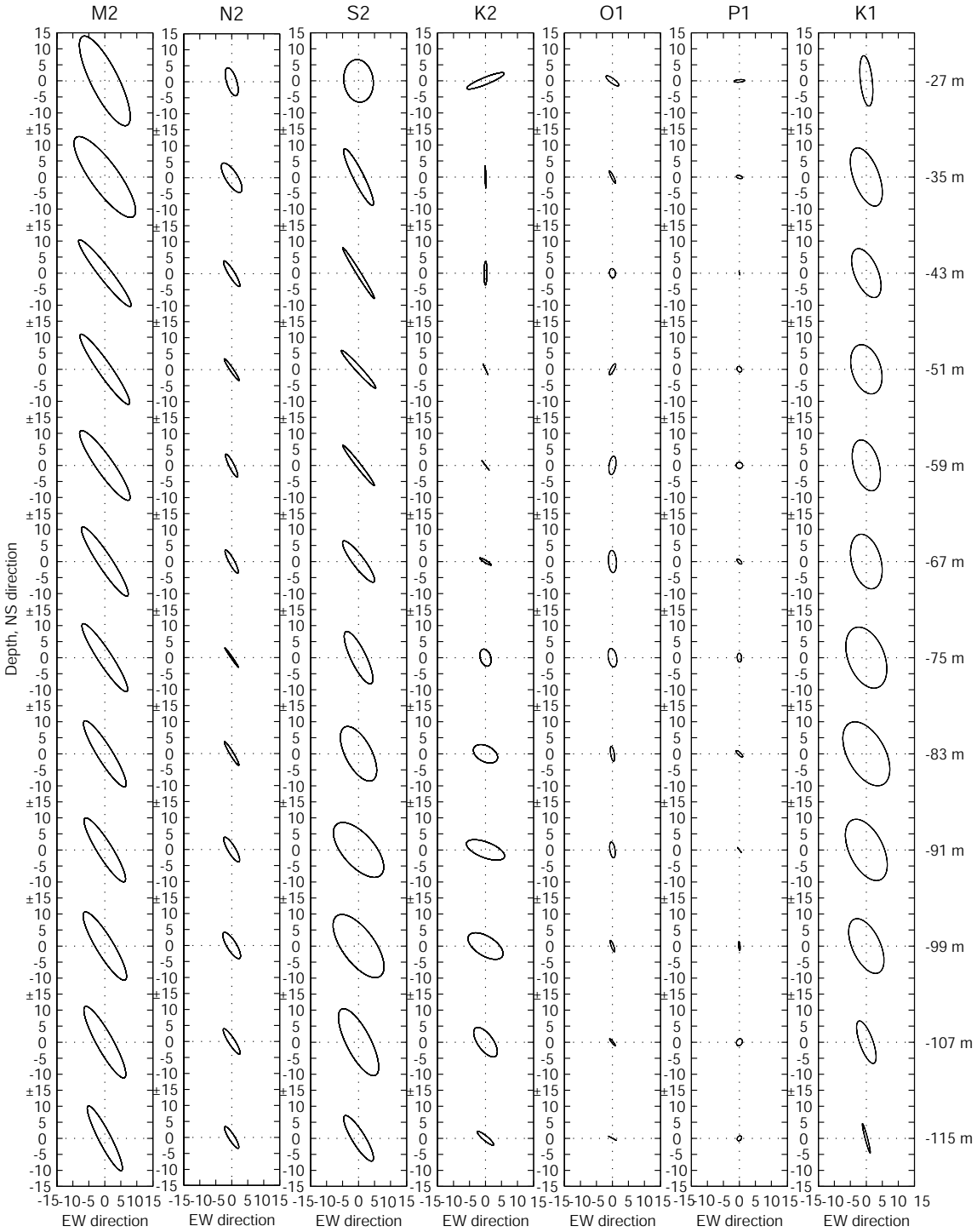


Figure 14: Current ellipses for the seven major tidal components (M2, S2, N2, K2, O1, P1 and K1) obtained by harmonic analysis of D1 measurements. Vertical spacing is 8m.

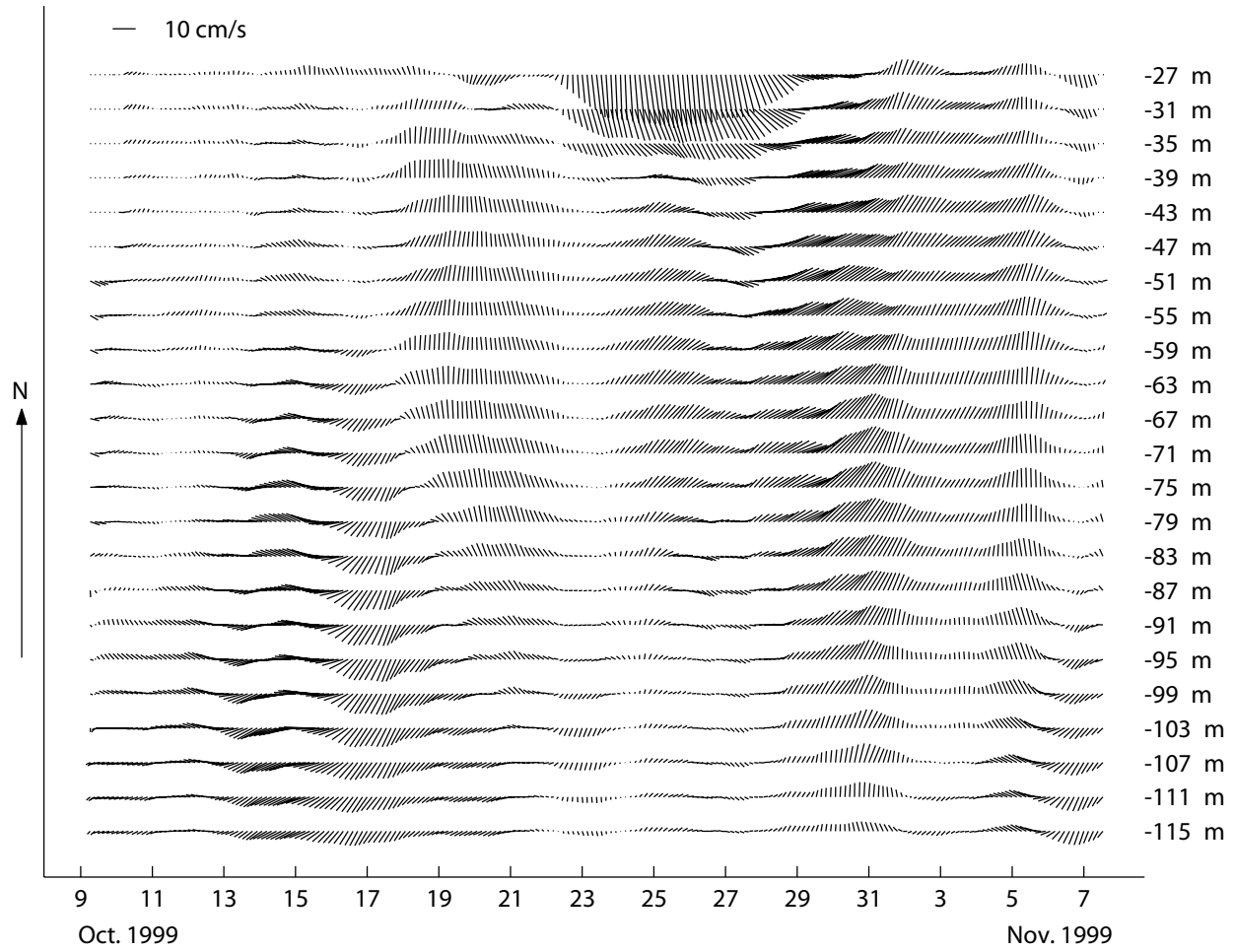


Figure 15: Time series of residual velocity at mooring D1 with 4m vertical spacing. The data have been filtered with a 25 hour low pass filter and have been resampled every 3 hours.

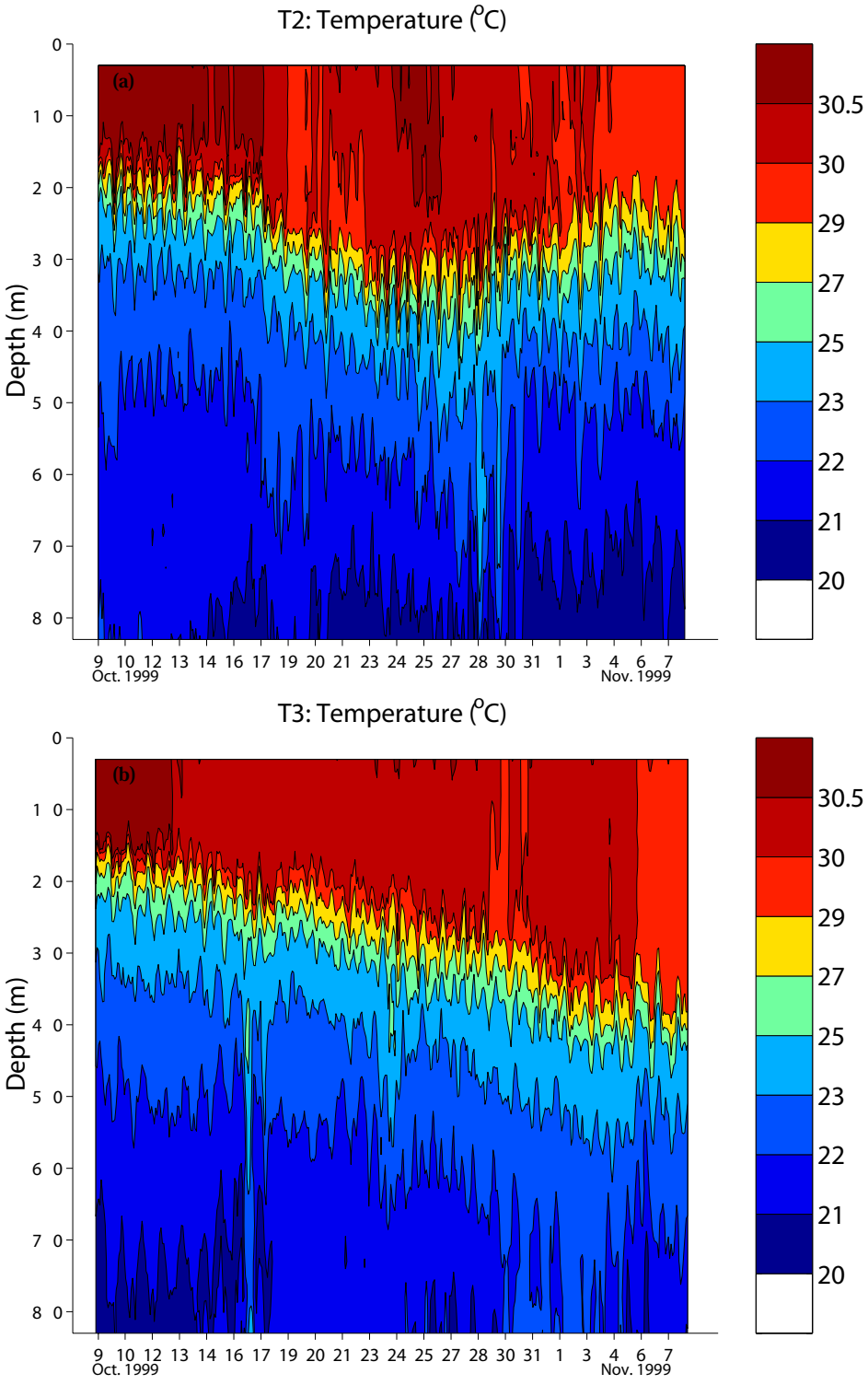




Figure 16: Time series of temperature profiles at T2 and T3 moorings. The data have been resampled every 100 minutes.

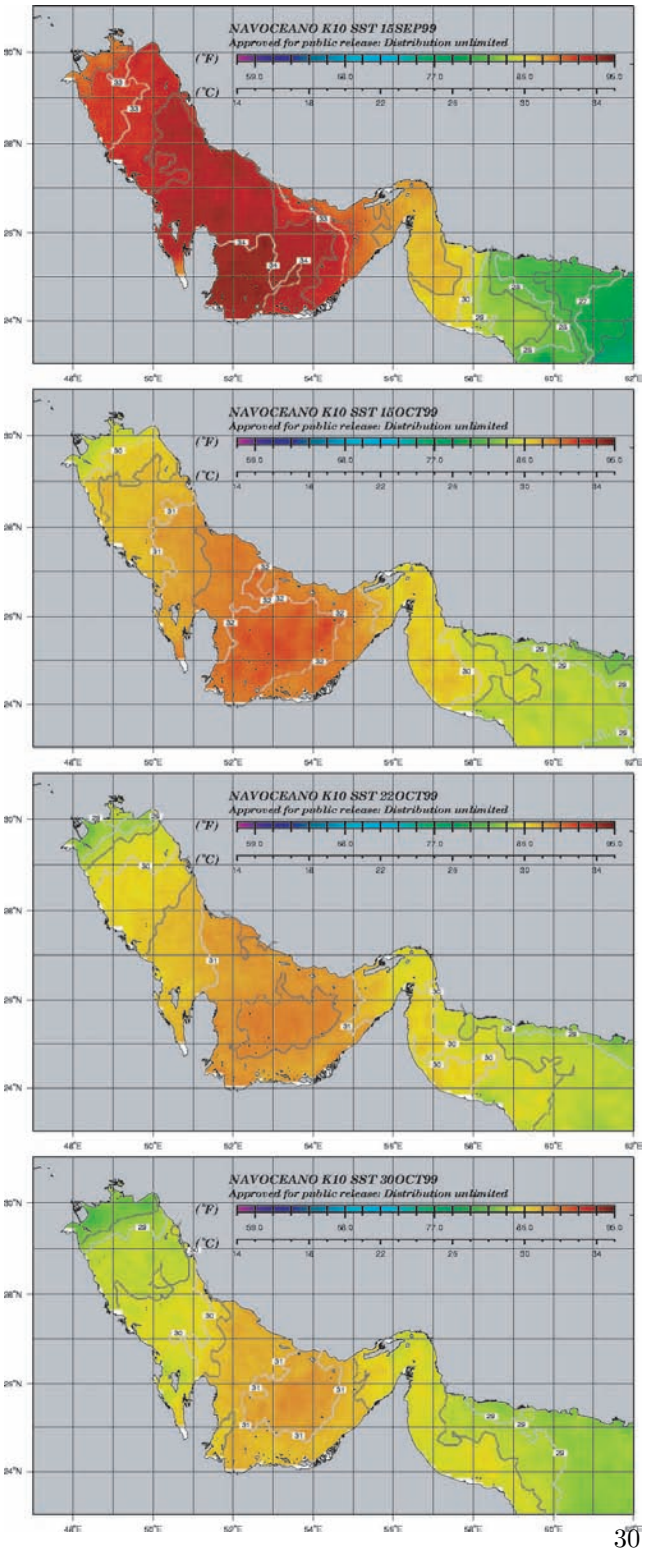




Figure 17: Composite K10 SST maps from NAVOCEANO on the two gulfs, at dates 09/15, 10/15, 10/22, 10/30, 1999.

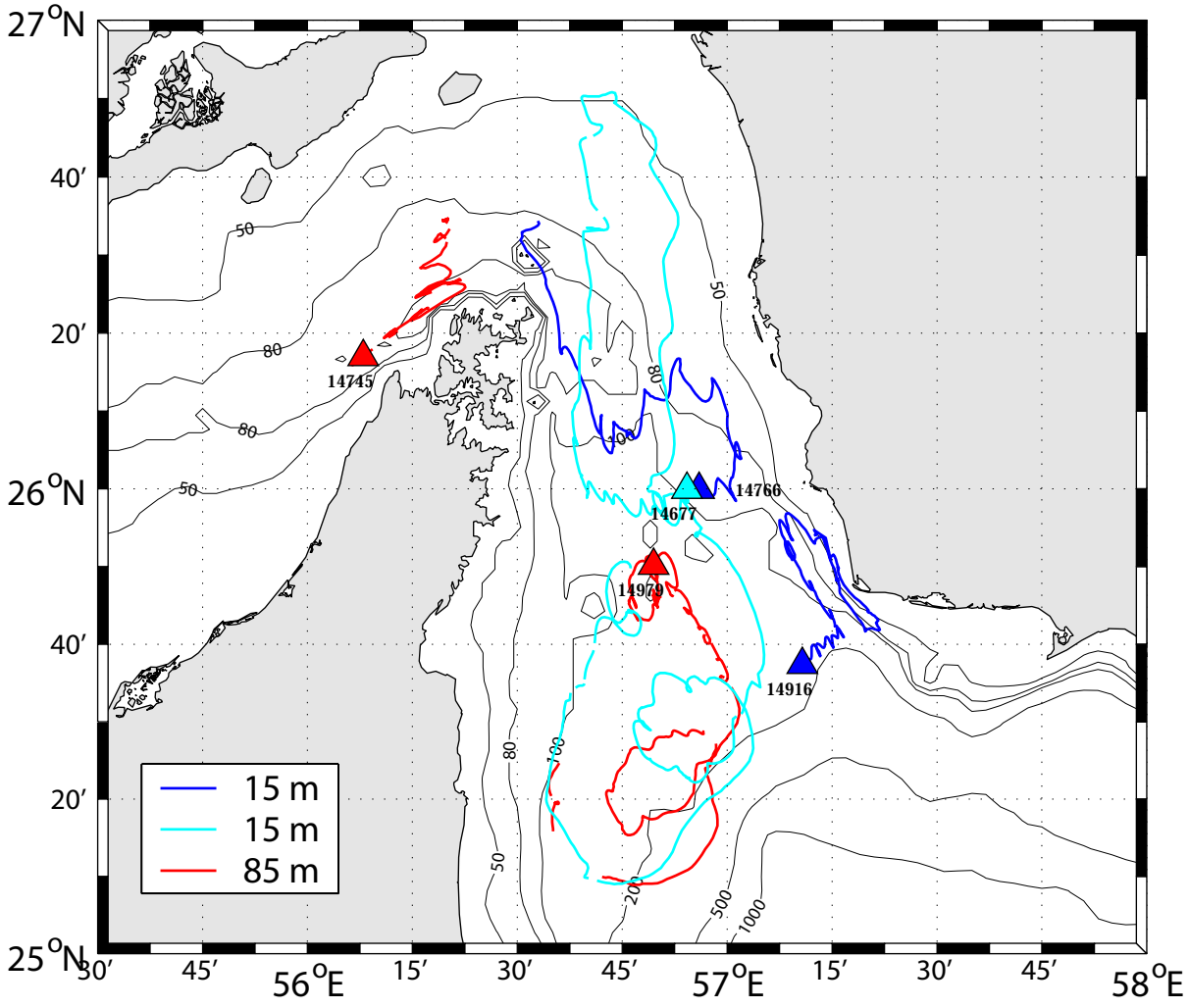


Figure 18: Surdrift buoy trajectories. Triangles indicate deployment position and colors give the drogue depth. Number of days of data is given in Table 3.